Eur Biophys J (1994) 23:1–19

European Biophysics Journal

Invited Review

Mechanosensitivity of cell membranes

Ion channels, lipid matrix and cytoskeleton

Alexander G. Petrov [1], **Peter N. R. Usherwood** [2]

[1] Biomolecular Layers Department, Institute of Solid State Physics, Bulgarian Academy of Sciences, 72 Tzarigradsko chaussee, BG-1784 Sofia, Bulgaria
[2] Department of Life Science, Nottingham University, University Park, Nottingham NG7 2RD, UK

Received: 9 June 1993 / Accepted in revised form: 19 October 1993

Abstract. Physical and biophysical mechanisms of mechano-sensitivity of cell membranes are reviewed. The possible roles of the lipid matrix and of the cytoskeleton in membrane mechanoreception are discussed. Techniques for generation of static strains and dynamic curvatures of membrane patches are considered. A unified model for stress-activated and stress-inactivated ion channels under static strains is described. A review of work on stress-sensitive pores in lipid-peptide model membranes is presented. The possible role of flexoelectricity in mechano-electric transduction, e.g. in auditory receptors is discussed. Studies of flexoelectricity in model lipid membranes, lipid-peptide membranes and natural membranes containing ion channels are reviewed. Finally, possible applications in molecular electronics of mechanosensors employing some of the recognized principles of mechano-electric transduction in natural membranes are discussed.

Key words: Mechanosensitivity – Mechanotransduction – Cell membrane complex – Ion channels – Modelling of stress-sensitivity – Lipid matrix – Cytoskeleton – Mechano-electric phenomena – Flexoelectricity – Model membranes – Mechanosensors

1. Introduction

Mechanosensitivity is a phenomenon which enables living systems to perceive and to react to mechanical stimuli, i.e. stress, strain, pressure (mechanical and osmotic), shear forces, acceleration, vibration, sound etc. At the level of the cell, studies of mechanosensitivity tend to concentrate on the membrane bilayer and its associated cytoskeleton. Here the principal problem is to define the exact location of the mechanosensitive centre, its molecular structure and its mechanical properties. Unfortunately, there is no consensus concerning the effects of mechanical deformation on biological macromolecules. Even the concept of mechanical degree(s) of freedom at the level of a single macromolecule is problematic. Such a concept requires the existence of a slowly relaxing set of conformational states (the 'molecular machine' of Blumenfeld 1974). However, there is a well-developed theoretical approach to the continuum properties of membrane bilayers based on liquid crystal physics (Helfrich 1973; Petrov et al. 1976, 1979, 1984; Sackmann 1978, 1983, 1984). This application of liquid crystal theory to membranology is very suitable for describing the electrical and mechanical phenomena associated with mechanoreception, and it has led to a better understanding of the relationships between the macroscopic and molecular properties of biological membranes (Petrov and Bivas 1984). Also, ideas from polymer physics have increased our understanding of the cell cytoskeleton (Schmidt et al. 1989) and its mechanochemical interactions with membrane bilayers (Sackmann 1984; Duwe et al. 1989).

This review begins with a description of some basic mechanisms, which, in principle, could be involved in mechanoreception. It will then pursue the manifestation of these mechanisms in model and living systems. It will be shown that important mechanical degrees of freedom may be provided by either the membrane bilayer and/or the cytoskeleton. Several reviews on this subject are already available (Sachs 1986, 1987, 1988, 1989; Morris 1990; Lecar and Morris 1993), including two comprehensive reviews on cell mechanotransduction with respect to hearing (Passechnik 1988; Howard et al. 1988).

2. Physical and biophysical mechanisms of mechanosensitivity

Since deformation is the primary effect of applying a mechanical force to a cell membrane, we shall present a brief

Dedicated to Professor Alexander Derzhanski on the occasion of his 60th birthday

Abbreviations: BLM, bilayer lipid membrane; SAC, stress-activated channel; SIC, stress-inactivated channel; MCYST, microcystin-LR; DPhL, diphytanoyl lecithin; CME, condenser microphone effect

Correspondence to: A. G. Petrov

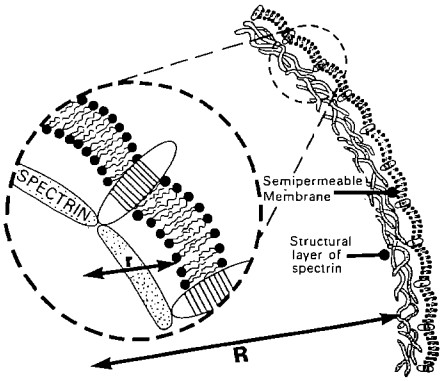

Fig. 1. Cartoon of membrane bilayer and the associated cytoskeleton (spectrin in the case of erythrocytes). The lipid bilayer is interspersed with integral proteins which are the anchorage points for the structural layer of spectrin. The model demonstrates that, even though the membrane as a whole may sustain a large tension (i.e. resist a hydrostatic pressure difference with a region of low curvature, of radius R), the lipid bilayer of the membrane (with much higher curvature, of radius r) may be subject to a lower tension (from Gruen and Wolfe 1982, with permission)

review of the elastic properties of membrane bilayers. The viscous properties of such structures involve irreversible changes and, therefore, are probably of less importance to mechanosensitivity, although viscoelastic properties may govern the frequency response of some complex mechanosensors (Passechnik 1988).

Biological membranes possess unique mechanical properties as a result of their laminar composite structure (Fig. 1) combining two states of matter: the liquid crystal membrane bilayer and the polymer network of cytoskeleton (Sackmann et al. 1989; Duwe et al. 1989). A typical, 5 nm thick membrane bilayer contains various integral proteins which may traverse the bilayer. Attached to these transmembrane macromolecules there is a quasi two-dimensional, filamentous network of peripheral membrane proteins, which comprise the cytoskeleton. In the erythrocyte membrane these proteins are spectrin and actin. The spectrin filaments are parallel dimers ~ 110 nm in contour length, which self-associate and/or couple to proteins, like ankyrin, to form tetramers. These are interconnected by actin oligomers to form a nearly hexagonal network (Sackmann et al. 1989). The cytoskeleton connects to the inner face of the membrane bilayer by binding to the integral proteins that it contains via ankyrin or other coupling proteins. Thus, the cytoskeleton forms a tension-bearing and tension-collecting framework for transmitting tension to the proteins of the bilayer, but only at its attachment points, which are spaced ~ 100 nm from each other (Sachs 1986).

2.1. Membrane elasticity

2.1.1. Membrane tension and tension-free membrane state. The fact that the membrane bilayer acts as a selective barrier for solute permeation introduces a potential source of membrane-related force, namely membrane tension. According to the Laplace law, in an inextensible membrane a hydrostatic pressure difference p across the membrane creates a lateral membrane tension T_m depending on the degree of curvature of the bilayer:

$$p = T_m (1/R_1 + 1/R_2), \tag{1}$$

where R_1 and R_2 are the two principal radii of curvature of the membrane. Thus, for a spherical membrane surface of radius R, the resultant tension $T_m = pR/2$ is higher when the radius of curvature is larger. The equivalent osmotic pressure difference in the case of a non-permeable solute present on one side of the membrane only at molar concentration c is, according to van't Hoff's law, $p = c\,\mathrm{R}\,T$, where R is the gas constant and T is the absolute temperature.

At this point, an important function of the cytoskeleton becomes clear (Fig. 1, Gruen and Wolfe 1982). Increased membrane curvature of a bilayer, between the points of attachment of the cytoskeleton, reduces membrane tension. This aspect of membrane-cytoskeleton interaction (called 'excess bilayer area model' is well established for erythrocyte membranes (Zeman et al. 1990, Fig. 12)). Though the membrane sustains a global tension of $pR/2$, this is supported by the cross-linking of the relatively rigid cytoskeleton. The lipid bilayer, which has a high curvature locally, sustains a tension of only $pr/2$, where r is the distance between the points of attachment of the cytoskeleton. For a typical cell $r/R \sim 0.01$; a substantial reduction of local tension being induced by the cytoskeleton (see below).

2.1.2. Area elasticity, compression elasticity, shear elasticity. In an elastic membrane, an isotropic lateral tension T_m will produce a proportional change (ΔA) in membrane area A. The relationship between ΔA and T_m (Hooke's law) involves an elastic coefficient K_a, the area elasticity modulus (Evans and Hochmuth 1978); viz

$$T_m = K_a (\Delta A/A), \tag{2}$$

where A is the initial membrane area.

If a uniaxial stress T_d is applied across a membrane it will produce a thickness change Δd which enters the definition of another elastic coefficient, the thickness elasticity modulus K_d (Evans and Hochmuth 1978):

$$T_d = K_d (\Delta d/d), \tag{3}$$

where d is the initial membrane thickness.

Because the hydrocarbon core of a membrane bilayer is almost incompressible by volume, i.e. a fractional area change produces an equal in absolute value and opposite in sign fraction thickness change the two elasticity moduli of a lipid bilayer are related by a simple relationship (Evans and Hochmuth 1978):

$$K_d = (1/d)\, K_a. \tag{4}$$

If a membrane is subjected to a uni-axial lateral tension T_1 and a uni-axial extension ΔL occurs whilst the total membrane area is conserved, then the so-called shear elastic modulus μ will govern the relationship between the shear resultant $T_s = T_1/2$ and the shear strain expressed in terms of the extensional ratio $\lambda = (\Delta L + L)/L$, where L is the initial length (Evans and Hochmuth 1978):

$$T_s = (1/2)\,\mu\,(\lambda^2 + \lambda^{-2}). \tag{5}$$

When a pure lipid bilayer is at a temperature above its main phase transition temperature it behaves as a two-dimensional liquid and does not display shear rigidity. However, the cytoskeleton does behave like a solid-like medium and, consequently, it has a non-zero shear elastic modulus. For example, $\mu = 6.6 \times 10^{-3}$ mN/m for the erythrocyte membrane (Waugh and Evans 1979). The cytoskeleton also makes an important contribution to the area elasticity modulus K_a. This modulus for an egg lecithin bilayer is 140 mN/m (Kwok and Evans 1979). A surprisingly low value for the area elasticity modulus of cultured chick muscle cell membrane has been reported, i.e. $K_a = 48.3$ mN/m (Sokabe et al. 1991). It is believed to represent the cytoskeletal elasticity only.

2.1.3. Curvature elasticity. Force couples (or torques) M acting across a membrane bilayer can create membrane curvature. According to Evans and Hochmuth (1978) this involves a curvature elasticity modulus K_c, viz

$$M = K_c (1/R_1 + 1/R_2 - 1/R_0), \tag{6}$$

where R_1 and R_2 are the principal radii of curvature of the membrane surface and R_0 is the initial or 'spontaneous' (Helfrich 1973) membrane curvature. Because of the thinness of a membrane bilayer, values for K_c are low; i.e. 1.15×10^{-19} J for a DMPC bilayer in a vesicle (Duwe et al. 1987; Duwe 1989), 0.43×10^{-19} J for a egg lecithin bilayer in a vesicle (Mitov et al. 1992), 0.56×10^{-19} J for a DMPC bilayer in a vesicle (Evans and Rawicz 1990); and 0.7×10^{-19} J for an erythrocyte membrane (Brochard and Lennon 1975) (see the comments in Petrov and Bivas (1984) and the recalculated value); Lennon 1977; Duwe et al. 1987). No clear influence of the cytoskeleton on K_c could be inferred from a comparison of pure lipid bilayers and biomembranes (Evans and Needham 1986). Measurements of intact erythrocyte membranes and haemolysed erythrocyte ghosts by Zilker et al. (1987) indicate a two-fold decrease of K_c after spectrin disruption. The smallness of the bending stiffness of a bilayer makes curvature deformation a promising candidate for mechanoreception (see below). However, such a system will be noisy because of thermally induced curvature fluctuations (e.g. Petrov and Bivas 1984) of the membrane surface.

2.2. *Mechanisms for conversion of mechanical stimuli into electrical signals*

Most of the information reviewed below was obtained from studies of model membrane systems.

2.2.1. Membrane capacitance variation. This is probably the simplest possible mechanism for mechanoreception. By stretching a membrane bilayer and, thereby, increasing its area (simultaneously decreasing its thickness if there is no lipid reservoir) the membrane capacitance C will be increased. If the membrane is clamped at a holding potential V, a capacitance current will flow across the bilayer. If a membrane is subjected to oscillating deformations its initial capacitance C_0 will be time-modulated as $C_0 + \Delta C \sin^2 \omega t$. The capacitative current will now be:

$$I = V \, dC/dt = \omega \Delta C \, V \sin 2\omega t . \tag{7}$$

This response to oscillatory inputs may be called the 'condenser microphone effect' (CME). It was discovered by Ochs and Burton (1974) and its frequency and temperature dependence was studied by Szekely and Morash (1980). A characteristic feature of CME is the frequency doubling of current when a membrane subjected to oscillating hydrostatic pressure is flat in its equilibrium position (cf. Eq. (7)). This doubling is either reduced or abolished by precurving the membrane. CME may have implications for mechanoreceptors in general (Ochs and Burton 1974).

2.2.2. Membrane conductance variation. Reversible conductance changes induced by hydrostatic pressure in black lipid membranes (BLMs) comprising lipid extracts from ox brain gray matter and toad urinary bladder were observed by Parisi and Rivas (1971). A reversible third power function between the applied pressure and the increase in conductance was found. Pressure is known to modify the electrical properties of toad bladder, and BLMs produced from lipids extracted from this tissue exhibited a 10-fold greater sensitivity to pressure than BLMs formed from ox brain lipids. A transient conductance change was observed above a certain threshold, suggesting a stretch-dependent modification of BLM structure. A more detailed discussion of pressure-driven currents in channel-containing bilayers is presented in Sect. 2.2.7.

Passechnik and Sokolov (1973), Bograchova et al. (1974) and Passechnik (1983) have studied the influence of periodic stretch (induced by oscillating pressure difference) on the conductivity of BLMs. The membranes contained low molecular weight ion carriers (ionophores) such as dibarenyl mercury (anion carrier), pentachlorphenol and tetrachlortrifluormethylbenzimidazole (proton carriers). A conductivity increase proportional to the pressure-induced increase in membrane area was observed in each case. Frequency doubling was again observed with flat (as opposed to pre-curved) membranes. The increase in conductivity was oscillation frequency-independent in the range 1 to 150 Hz. A mechanosensitivity coefficient was defined as the ratio of the relative conductance change $\Delta G/G$ and the relative area change $\Delta A/A$. It was found to be frequency-independent, with a numerical value in the range of 40. In order to account for the conductance increase, a stretch-induced change in the distribution coefficient of the ionophore between the peripheral and central regions of the BLM was proposed. This change was thought to be due to a position-dependent interaction of ionophore with bilayer.

2.2.3. Flexoelectricity. This is a direct mechanism for transformation of mechanical stimuli into electrical signals. Flexoelectricity results from curvature-induced membrane polarization (Petrov 1975; Petrov and Bivas 1984):

$$P_s = f (1/R_1 + 1/R_2), \tag{8}$$

where P_s is the electric polarization per *unit area* in C/m and f is the flexoelectric coefficient in C (coulombs) (note the formal analogy between the constitutive equation (8) and the Laplace law (1)). Flexoelectricity is manifested in liquid crystals and liquid crystalline membrane structures where curvature causes an orientational splay deformation of the membrane constituents (cf. Meyer 1969). As with piezoelectricity in solid crystals, flexoelectricity can also be manifested by of direct flexoelectric effect (i.e. curvature-induced polarization, Eq. (8)) and by of converse flexoelectric effect (i.e. an electric field-induced curvature, Eq. (9) (Todorov et al., submitted):

$$(1/R_1+1/R_2)=(f/K_c)\,E\,, \tag{9}$$

where E is the transmembrane electric field and K_c is the curvature elasticity modulus (see Eq. (6)). Equation (9) is valid for a tension-free membrane (of zero lateral tension).

The phenomenon of flexoelectricity has been studied extensively, theoretically and experimentally (Petrov and Derzhanski 1976; Petrov 1978; Petrov et al. 1979; Petrov 1984; Derzhanski et al. 1990; Petrov 1992). Theoretical results reveal the important contribution of the longitudinal component of the lipid dipole moments (μ) and partial surface charges (βe, where β is the degree of ionization and e is the proton charge) of the lipid head groups. For a symmetric bilayer, the dipolar part of the flexoelectric coefficient f^D, when lateral exchange of lipids between regions of different membrane curvature is blocked (high frequency regime of curvature oscillation), is (Derzhanski et al. 1989, 1990):

$$f^D=[(\mu/A_0)-(\mathrm{d}\mu/\mathrm{d}A)_0]\,d\,, \tag{10}$$

where A_0 is the area per lipid head in flat membrane state and $(\mathrm{d}\mu/\mathrm{d}A)_0$ is the derivative of the dipolar moment with respect to the area at A_0. When free lateral exchange of lipids is allowed (low frequency oscillations or static curvature) the membrane thickness d in (10) is replaced by the (shorter) distance $2\delta_H$ between the neutral surface of a monolayer and the head group surface (Petrov and Bivas 1984). The surface charge part of the flexoelectric coefficient f^C is easily obtained from (10) by substituting μ by the dipolar moment of the diffuse electric double layer $\beta e \lambda_D$ (Petrov 1992):

$$f^C=e[(\beta/A_0)-(\mathrm{d}\beta/\mathrm{d}A)_0]\,\lambda_D(d+\lambda_D)\,, \tag{11}$$

where λ_D is the Debye length, which depends on the inverse of the square root of counterion concentration. A quadrupolar contribution to the flexoelectric coefficient is also conceivable. It would be negligible for membrane lipids, but dominant for closely-packed and uniaxially-ordered integral membrane proteins (Petrov 1984). Free, laterally diffusing membrane proteins can also contribute to the flexoelectric coefficient (by their longitudinal dipole moments and their shape asymmetries), by virtue of their accumulation in the curved membrane regions (Petrov 1984). The cytoskeleton could also play an active role in inducing membrane curvature, e.g. by an ATP-induced spectrin contraction (Petrov 1978).

Flexoelectricity can be studied experimentally by using oscillating pressure (Petrov and Sokolov 1986), e.g. by using a BLM which is forced to oscillate viz:

$$(2/R)=(2/R_c)\sin\omega t\,, \tag{12}$$

where $(2/R_c)$ is the curvature amplitude. This approach was recently used also to study flexoelectricity in lipid bilayers and biomembranes attached to the tips of patch pipettes (Petrov et al. 1989). A high input impedance electrometric amplifier was used to register transmembrane voltage changes due to P_s:

$$U=(1/\varepsilon_0)\,(f^D/\varepsilon_L+f^C/\varepsilon_w)\,(2/R_c)\sin\omega t\,, \tag{13}$$

where ε_L is the dielectric constant of the lipid core, ε_w is the dielectric constant of water in the electrical double layer region at the membrane/solution interface and ε_0 is the absolute dielectric permeability of free space. A low input impedance amplifier was used to measure the displacement current induced by variations of P_s. When lateral exchange of lipid in the bilayer is blocked the flexoelectric current is (Petrov 1992):

$$I=\frac{f^D+(\varepsilon_L/\varepsilon_w)\,f^C}{d+(\varepsilon_L/\varepsilon_w)\,2\lambda_D}\,S(2/R_c)\,\omega\cos\omega t\,, \tag{14}$$

where S is the membrane area.

The amplitude of the membrane curvature $(2/R_c)$ can be estimated electrically using the CME (Eq. (7)) (Ochs and Burton 1975; Petrov and Sokolov 1986). Very recently, a direct interferometric method under stroboscopic laser light illumination was developed, allowing for a precise determination of R_1 and R_2 (Todorov et al. 1991).

Experimental data on flexoelectricity in BLMs of various lipids and various ionic environments were reviewed by Petrov (1992). For a BLM of glyceryl monooleate, a non-charged lipid, f was 3×10^{-20} C. This low value is expected for such a membrane featuring dipolar contribution only (10) (Todorov et al. 1991). For BLMs comprising weakly-charged phospholipids of biological origin (egg lecithin, *E. coli* ethanolamine) f is much higher, i.e. 10^{-18} C (Petrov and Sokolov 1986; Derzhanski et al. 1990; Todorov et al. 1991). Preliminary measurements of flexoelectricity in membrane patches excised from locust muscle give values for f of about 10^{-20} C (Petrov et al. 1993). Assuming this to be a correct estimate, then with a membrane patch of radius 100 nm (the estimated distance between the points of attachment of the cytoskeleton (Fig. 1)) a transmembrane voltage of 23 mV would be induced according to (13) (where f equals the total expression in the brackets). To produce this membrane voltage, the cytoskeleton must consume energy (e.g. ATP chemical energy) equal to the curvature elastic energy of $4\pi K_c$ for a hemispherical patch, i.e. 8.8×10^{-19} $I=220\,k_B\,T$ (k_B is Boltzman constant).

2.2.4. Piezoelectricity. This phenomenon is only manifested in ordered structures which lack a centre of symmetry. This condition is fulfilled with nonsymmetric bilayers, i.e. those constructed from monolayers of different lipid composition. This situation is typical for biomembranes. Here the surface polarization of a flat membrane P_{S0} may be nonzero and stretch-dependent (Petrov 1986):

$$P_S=P_{S0}+e_S\,(\Delta A/A)\,, \tag{15}$$

where e_S is a piezoelectric coefficient in C/m. Molecular considerations (Petrov 1986) give an expression for e_S in terms of the area derivatives of the dipolar moments of the outer (o) and inner (i) monolayers, where both permanent dipole moments and electrical double layers dipole moments are considered (cf. (10) and (11)):

$$e_s=(\mathrm{d}\mu^o/\mathrm{d}A)_0-(\mathrm{d}\mu^i/\mathrm{d}A)_0\,, \tag{16}$$

the derivatives being taken again at A_0, the mean area per lipid head in flat membrane state. Estimates based on surface potential measurements of lipid monolayers suggest a value of 10^{-12} C/m. With a relative area change of 1% (close to the lytic limit) the calculated change in transmembrane voltage is 1 mV. Unfortunately, there are no experimental data to test this conclusion. In principle, a shear piezoelectricity could also be envisaged for biomembranes because of the cytoskeleton.

Another mechanism of membrane piezoelectricity may be provided by permanent ferroelectric polarization in biomembranes. Beresnev et al. (1982) postulated the occurrence of ferroelectricity in liquid crystal type membranes with tilted lipid chains containing chiral molecules (cholesterol etc.). Recently, Petrov et al. (1991 b) demonstrated ferroelectric polarization in lamellar liquid crystal phases of dipalmitoyl lecithin-cholesterol using an oscillating drop technique. Here, the piezoelectric signal was obtained in the tilted gel and ripple phases only. The ferroelectricity produces a permanent polarization parallel to the membrane plane and normal to the tilt plane. A tilt may exist locally even in the fluid phase due to the integral membrane proteins. When the tilt angle is modulated mechanically, e.g. by a shear force (as in the experiment of Petrov et al. 1991 b), the in-plane polarization is also modulated and depolarizing currents are induced along the two membrane surfaces.

2.2.5. Pore formation in the lipid bilayer. Possible mechanisms underlying flexoelectricity that have been considered so far, have neither implied the existence of conducting pathways or defects in the membrane bilayer nor their emergence under mechanical stress. Instead, the bilayers were considered as elastic, two-dimensional continua. However, the structural and functional properties of membrane channels may also be stress-sensitive.

The subject of pore formation during application of lateral tension to membrane bilayers has been earlier reviewed by Petrov et al. (1980). Litster's (1975) idea of a semi-toroidal pore structure and his theoretical approach based upon the concept of a line energy per unit length of the pore edge, called 'edge energy' have been developed to include the dependence of the edge energy on the pore radius R (see also Petrov et al. 1991 a). The concept of generalized molecular asymmetry (Derzhanski and Petrov 1982; Petrov and Derzhanski 1987; Petrov 1988), specifically the biphilic and shape asymmetry of membrane lipids, was used to show how wedge-shaped lipids (lysophospholipids, free fatty acids, glycolipids, gangliosides etc.), by virtue of their accumulation in the strongly curved lipid monolayer part of the edge (Fig. 2b), decrease the edge energy and promote pore opening. They do this by accumulating in the strongly-

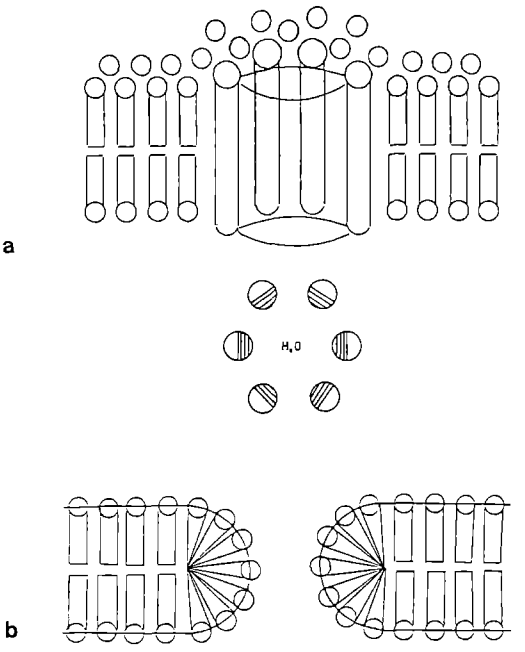

Fig. 2a, b. Two types of aggregation of conductive defect-forming molecules in lipid bilayer membranes according to their shape asymmetry and biphilic asymmetry: **a** channel, an aggregate of cylindric molecules featuring transversal biphilic asymmetry (hydrophilic portions hatched). Molecular length should roughly match the bilayer thickness. **b** pore, an aggregate of wedge-shaped molecules featuring longitudinal biphilic asymmetric. Molecular lengths should roughly match half of a bilayer thickness (from Petrov et al. 1991 a)

curved part of the membrane surface lining the pore. Assuming the series expansion:

$$\gamma(R)=\gamma_0+\gamma_1/R+\gamma_2/R^2\,, \tag{17}$$

the pore radius $R_0=\gamma_2/\gamma_0$ in the unstressed bilayer was calculated and its increment ΔR caused by application of lateral tension T_m to the bilayer was determined from (Petrov et al. 1991 a):

$$\Delta R=T_m R_0^2\,(2\gamma_0-3\,T_m\,R_0)^{-1}\,. \tag{18}$$

When T_m is low, ΔR increases linearly with T_m. However, the concomitant conductance increase might initially be nonlinear, because very narrow pores may be nonconducting (Pastushenko and Petrov 1984). When T_m approaches the critical tension $T_{cr}=2\gamma_0/3R_0$, there is an irreversible growth of the pore leading to disruption of the bilayer. Molecular modelling provides specific values for γ_0, γ_1 and γ_2 (Petrov et al. 1980). γ_0 has been estimated experimentally only for egg lecithin. Its experimental value is 2×10^{-11} J/m (Harbich and Helfrich 1979). Wedge-like molecules decrease this value. With a pore radius of 1 nm, the critical tension is of the order of 10 mN/m.

An alternative approach is to imagine a membrane pore as a multimer of asymmetrically-shaped monomeric lipids (Petrov 1981). An analogous type of organisation could also account for pores generated in bilayers seeded with certain toxic oligopeptides (e.g. melitin, microcystin (Petrov et al. 1991 a)). Here the pores would be expected to be semi-toroidal.

2.2.6. Ion channels. Some transmembrane proteins have integral ion channels which can, in part, be modelled using synthetic helical polypeptides (Fig. 2a) (Sansom 1991). The biphilic asymmetry for the type of aggregates formed by these proteins and peptides was described precisely by Brasseur (1991) using molecular hydrophobicity potential calculations. However, the edge energy concept is general enough to describe the stress-sensitivity of membrane pores and channels, providing its parameters are quantified by specific molecular modelling, although it is important to note that openings of pores and channels by lateral tension would not be a continuous process (cf. Eq. (18). In the case of pore formation it would be a stepwise process, with each step requiring the recruitment of a new monomer molecule to the multimer lining the pore (either lipid or peptide). Pore formation is also promoted by transmembrane voltage, i.e. electroporation (Neumann et al. 1989).

Mechanical regulation of the activity of an ion channel relies on the existence of slowly relaxing, mechanical degrees of freedom in such an integral protein molecule. It requires two conditions (Howard et al. 1988). First, a force must be exerted on the membrane protein through an elastic element which is tensed by displacement. Second, a change in channel activity must entail a change in conformation that alters the tension in the elastic element. A two-state model of this type was proposed for displacement-sensitive hair cells by Howard et al. (1988). The tip links between adjacent stereocilia (Fig. 3) may serve as gating springs. The energy difference between open (o) and closed (c) states of the channel was obtained as:

$$\Delta g = g_o - g_c = -k_G x d + \mu_o - \mu_c , \tag{19}$$

where k_G is the spring stiffness, d is the gating distance, i.e. the difference in spring length between the open and closed states, x is the extension of the gating spring when the channel is midway between its open and closed states and μ_c (μ_o) is the molecular free energy of the closed (open) channel with no tension in the spring. From Boltzmann's law, the probability of finding the channel in the open state when the system is in equilibrium is:

$$P_{op} = (1 + \exp(\Delta g / k_B T))^{-1} . \tag{20}$$

P_{op} increases with x. In turn, this is coupled in the model of Howard et al. to the displacement of the stereocilia bundle. The sigmoidal curve expected from the Howard et al. model provides a good fit to the displacement-response relationship for bullfrog saccular hair cells (Howard et al. 1988). The gating spring stiffness is ~ 80 μN/m, while the gating distance is ~ 3.5 nm. Each channel is gated by a force of 40 fN. If the tip link (length ~ 100 nm; diameter ~ 5 nm) is to have the same stiffness as the gating spring its Young's modulus would have to be ~ 400 kPa, a value characteristic of resilient proteins such as elastin.

The Howard et al. (1988) model is analogous to the charge-displacement model for gating of voltage-sensitive channels in natural membranes, where $d(k_G x)$ in (19) is replaced by the product $q V$ of the gating charge and transmembrane potential.

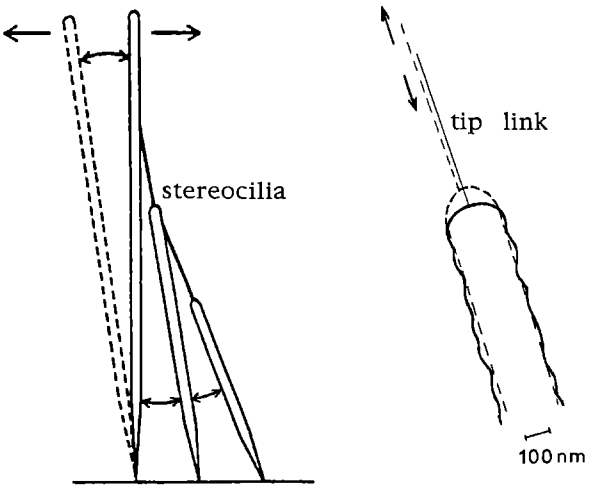

Fig. 3. A model for applying stress to the membranes of stereocylia in hair cells. The left panel shows how tilting of the bundle of cilia to the left (excitatory excursion) leads to stretching of the cilia membranes because of the pull exerted by the tip links. (For the implication of this observation on the stress-sensitive channel functioning see Sect. 2.2.6 and 4.2). The right panel shows that the tip curvature under excitatory/inhibitory tilt is increased/decreased. (For the implication of this observation on the flexoelectric sensing mechanism see Sect. 5.0)

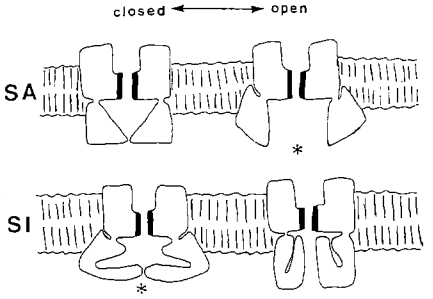

Fig. 4. A simplified elastic transduction model for stress-activated (SA) and stress-inactivated (SI) channels. The selectivity filter (black region) is unaffected by membrane tension. At any given tension, the channel is in thermal equilibrium between closed and open states but the closed/open probability is a function of membrane tension. The channel state favoured in the absence of stretch was considered to be more distensible and smaller in cross section, while the larger, stiffer state (asterisks) becomes more probable under stretch. This yielded a SA channel (small, soft closed state) and a SI channel (small, soft open state). (From Morris 1990, with permission). Quantitative expression of this model is given by Eq. (21).

Howard et al. (1988) generalized their model to embrace the stress-activated channels (SACs) discovered by Guharay and Sachs (1984) (see below). They replaced the gating spring by the lipid bilayer surrounding the channel and the gating distance by the difference in membrane area displaced by the open and closed channel conformations of a SAC (Fig. 4). The difference in area, ΔA_p, envisaged to be of molecular dimensions, would be multiplied by membrane tension T_m to produce a difference in energy between the open and closed states:

$$\Delta g = -\Delta A_p T_m + \mu_o - \mu_c , \tag{21}$$

where μ_o (μ_c) is the molecular free energy of the open (closed) channel with no tension in the bilayer. The depenence of channel open probability on tension is sigmoidal (20) and when this relationship was applied to the experimental data of Guharay and Sachs (1984), Howard et al. (1988) estimated that the difference in the maximum cross-sectional area of the channel for the open and closed states of this channel is 4–8 nm^2 maximum. This is probably less than 10% of the total area A_p of the open channel. More specific estimates are presented below. The linear model of Howard et al. (1988) estimates a gating area three orders of magnitude smaller than that estimated by Guharay and Sachs (1984), who used a quadratic model. The difference between the linear and quadratric models is that in the former the probability of the channel being in its open state depends on the energy difference between its open and closed states at a given tension T_m, whereas in the quadratic model it depends on the energy difference between the open state at tension T_m and the open state at zero tension:

$$g = -(A_p/2K_a)\, T_m^2\,, \tag{22}$$

where A_p is the total gating area and K_a is the area elasticity modulus of the gating area (cf. 2). Using the area elasticity values presented above (Sect. 2.1.2), the gating area from the quadratic model is estimated to have a (rather substantial) radius of 60 to 500 nm, the upper value being more probable (Sachs 1986). This implies that the cytoskeleton must be involved in channel gating in order to collect stresses from an area much larger than the channel itself, and there must be an optimum channel density of $\sim 1\ \mu m^{-2}$. Sachs (1986) has suggested that displacement-sensitive channels are really stretch-activated channels, where displacement of the hair bundle changes the tension in the stereocilium membrane containing the channels (Fig. 3). In the linear model of Howard et al. (1988) the cytoskeleton may have a role in channel gating, but not necessarily so. It also predicts a higher density of SACs.

The linear model could also be a good descriptor of another class of mechanosensitive channels, i.e. the stress-inactivated channels (SICs) (Morris and Sigurdson 1989; Morris 1990). It suffices to suppose that the cross-section area of the open channel conformation of a SIC is smaller than that of the closed conformation ($\Delta A_p < 0$ in Eq. (21); this was forseen qualitatively by Morris (1990, see Fig. 4). In fact, if the cross-sectional areas of the open and closed states of a channel do not differ substantially then that channel would be stress-insensitive. Thus, a simple classification of the channels with respect to their stress sensitivity could be proposed.

Very recently, Sachs and Lecar (1991) considered the statistical mechanics of conformational transitions between two states of an elastic channel in the presence of an external force field. The results predict both linear and quadratic terms. The linear term is larger than the quadratic one. The actual contribution of the two terms must be evaluated experimentally by quantitative analysis of the force-response data, preferably from rate constants rather than probabilities (Sachs and Lecar 1991). Such data are not yet available.

Passechnik (1983, 1988) discussed the possibility of a channel in which the closed and open states differ in length rather than in cross-sectional area, so that an increment/decrement Δd ($>$ or <0) of the membrane bilayer thickness d_o is induced around the channel when it opens. Channels of the gramicidin type may fit into this category (Hladky and Haydon 1984; see 4.1). The increment in channel length is supposed to extend within a radius r_1 around the channel, r_1 being several times larger than the channel radius because of the collective liquid crystal properties of the lipid bilayer (Huang 1986). Recalling (2), (3) and (4) for a volume-incompressible membrane ($\Delta d/d = -\Delta A/A$):

$$\Delta g = -\Delta d\, T_d\, \pi r_1^2 + \mu_o - \mu_c = (\Delta d/d_o)\, T_m \pi\, r_1^2 + \mu_o - \mu_c\,. \tag{23}$$

Thus, channels with negative (resp. positive) Δd will be activated (resp. inactivated) by lateral tension T_m.

Passechnik (1983) also proposed a mechanism in which changes in channel conformation are coupled to membrane curvature. In this case, changes in channel cross-sectional area resulting from channel opening should perturbate only one half of the membrane bilayer (Passechnik 1988) viz:

$$\Delta g = -\Delta s\, K_c\, (1/R_1 + 1/R_2)\, \pi\, r_1^2 + \mu_o - \mu_c\,, \tag{24}$$

where s is the splay asymmetry of the channel, Δs is the splay asymmetry difference between the two states: $\Delta s = \Delta\alpha/2r$ ($\Delta\alpha$ being the wedge angle change and r, the outer channel radius), r_1 ($>r$) is the radius of the curved area of membrane around the channel (Petrov et al. 1979). Normally, Δg would be much less than $k_B\, T$, unless R approaches r_1 (e.g. the tip of a stereocilium).

The possible existence of shear stress-sensitive channels was raised by Olesen et al. (1988) and Morris (1990). In fact, the model of transduction within a single stereocilium proposed by Sachs (1986) as an alternative to the stereocilia bundle model, actually involves shear-stress sensitive channels, but also the cytoskeleton.

2.2.7. Pressure-driven currents. Before completing this review of biophysical models of mechanosensitivity, the notion of pressure-driven transmembrane ion currents should be raised. Assume a channel-containing membrane of maximum cross-sectional area A separating two symmetrical electrolytes (e.g. KCl) of molar concentration c and with an applied transmembrane pressure difference p. By using the non-equilibrium thermodynamics approach to ion transport (Katchalski and Curran 1965) and by combining the two Katchalski equations for pressure-driven solute flow of cations and anions through channels into one equation, the pressure-driven electric current I is defined as:

$$I = e\, c\, (\sigma_{Cl} - \sigma_K)\, L_p\, p\, A\,, \tag{25}$$

where e is the proton charge, σ_K is the reflection coefficient for cations (i.e. the proportion of the cationic current which is reflected away from the membrane), σ_{Cl} is the reflection coefficient for anions and L_p is the filtration coefficient. Depending on the ionic selectivity of a channel

(i.e. the sign of the difference between the reflection coefficients), the membrane current may be either in the direction of the applied pressure or opposite to it. A similar equation, for cations only, described in terms of a drag coefficient, was proposed by Passechnik and Bichkova (1978).

Reflection coefficients for ions are generally unavailable, but they are expected to be close to 1. Therefore, in the case of a cation-selective channel it can be assumed that $\sigma_{Cl}-\sigma_K<0.1$. Consider a hemispherical membrane patch of radius 1 μm and a large (nearly lytic) transmembrane pressure of 100 torr (1 torr = 1 mm Hg = 133 Pa). Using the value of the filtration coefficient for an erythrocyte membrane of 0.92×10^{-12} m^3 N^{-1} s^{-1} and a typical ion concentration of 0.15 mol/l = 0.9×10^{26} m^{-3}, Eq. (23) yields a pressure-driven current of 10^{-13} A. Such a small current could presumably be neglected when discussing mechanosensitivity. Thus, pressure-driven currents are unlikely to account for mechanosensitivity of membrane channels (Derzhanski et al. 1981). Sachs (1988) arrived at a similar conclusion based upon a comparison of the electrical and pressure forces acting on a single ion.

2.2.8. Comparison of different mechanisms. General comments. The problem of energy transformation in mechanoreceptors was addressed two decades ago (Passechnik 1972, 1974, 1977). Models of mechanosensitivity which are based upon stress-induced variations of membrane conductivity may be compared by examining their mechanosensitivity coefficients $\varkappa=(\Delta G/G)/\phi$, where ϕ is the relative displacement $(\Delta x/x)$, relative area change $(\Delta A/A)$, or the relative curvature change $(\Delta c/c)$ where appropriate. In the case of a continuously stretched pore changes in conductivity could be equated with changes in pore cross-sectional area (resp. pore radius). For a single channel conductivity G is proportional to the open state probability P_{op} (20). Then, assuming small mechanical deformations, so that $\Delta g<k_B T$, the general expression for $\varkappa$ is (Passechnik 1983, 1988):

$$\varkappa=-(\Delta g(\phi)-\Delta g(0))/k_B T, \tag{26}$$

where $\Delta g(\phi)-\Delta g(0)$ is the change in the difference between the free energies of the open and closed channel states due to the mechanical deformation (a factor of $(1+\exp(\Delta g(0)/k_B T)^{-1}\sim1/2$ being neglected in (26)). The results of this approach are as follows:

i) Continuously stretched pore. Using (18) and with a lipid bilayer area elasticity $K_a=140$ mN/m, pore radius $R=1$ nm and edge energy $\gamma_0=2\times10^{-11}$ N:

$$\varkappa=K_a R/\gamma_0=7$$

ii) Displacememt-sensitive channel. From (19, 26) and with gating distance $d=3.5$ nm and gating force $F_G=40$ fN:

$$\varkappa=d F_G/k_B T=35$$

iii) Area stress-sensitive channel (linear model). This model is characterized by a stress-independent sensitivity. From (21) and (26) with $K_a=140$ mN/m and $\Delta A_p=8$ mm^2:

$$\varkappa=K_a A_p/k_B T=280$$

iv) *Area stress-sensitive channel (quadratic model).* Stress-sensitivity in this model depends linearly on lateral stress T_m. From (22) and (26) with gating area $A_p=8\times10^5$ nm^2 and $T_m=1$ mN/m:

$$\varkappa=A_p T_m/2k_B T=10^5$$

v) Thickness stress-sensitive channel. From (23) and (26) with relative thickness deformation $\phi_d=\Delta d/d=0.1$, $K_a=140$ mN/m and disturbed area radius (after Huang 1986) $r_1=5$ nm:

$$\varkappa=\phi_d K_a \pi r_1^2/k_B T=280.$$

vi) Curvature-sensitive channel: Sensitivity in this model depends on the initial bilayer curvature $c_0=2/R_0$. From (24) and (26), assuming $R_0=r_1$, a wedge angle change $\Delta\alpha$ of 0.1 rad, and [disturbed area radius]/[channel radius] $=r_1/r=5$ and $K_c=1\times10^{-19}$ J:

$$\varkappa=K_c \Delta s\, c_0\, \pi r_1^2/k_B T=K_c \Delta\alpha\, \pi(r_1/r)/k_B T=40.$$

Experimentally evaluated values for mechanosensitivity coefficients, necessary to match the observations for various mechanoreceptors membranes should be 10^3–10^4 (Passechnik 1977), although in some cases values as low as 10^1 have been quoted (Passechnik 1983). These evaluations depend on many assumptions related to the unknown mode of deformation of hair cells and unknown location of mechanosensitive centers. Comparing our estimates for the area stress-sensitive channel and thickness stress-sensitive channel to the corresponding ones of Passechnik (1983, 1988) it is clear that the values estimated by us are one to two orders of magnitude lower. This is due mainly to the unrealistically high value of 5000 mN/m for area elasticity ($K_a=E\,d$, where E is Young modulus) that was used by Passechnik (1988). The experimentally-derived area elasticity for lipid bilayers is $K_a=140$ mN/m (Kwok and Evans 1981). An exceptionally high stress sensitivity is provided by the quadratic model, but only at a substantial initial stress level. This is related to its huge gating area compared to the linear model (see above). Nevertheless, the linear model has the advantage of providing a stress-independent sensitivity, even at very low stress, and a linear response. Moreover, this is the only model capable of describing the activities of both SACs and SICs in the same framework.

A continuously-stretched pore provides a much lower sensitivity to stress than a channel, where opening and closing results from conformational changes of a transmembrane protein (Passechnik 1983).

If a single protein molecule containing a channel is to provide acceptable values for the mechanosensitivity coefficient, it has to be an unrealistically large macromolecule. In other words, mechanosensitivity must involve other parts of the bilayer. The concept of a mechanosensitive centre comprising an ionic channel, exhibiting conductivity fluctuations, and its immediately adjacent membrane bilayer was first advanced by

Passechnik (1972). Following general principles (Blumenfeld 1974) it was envisaged as a lipid-protein system undergoing substantial changes in the free energies of its parts whilst keeping the total free energy of the system relatively unchanged (Passechnik 1977). The lipid bilayer (and the cytoskeleton) provides at least three important mechanical degrees of freedom which may be involved in mechanoreception: area, thickness and curvature.

The other cited mechanisms for direct transformation of mechanical stimuli into electrical responses (capacitance, flexoelectricity, piezoelectricity) are not comparable to models in which changes of membrane conductance are involved. However, the electromechanical coupling coefficient:

$f^2/\varepsilon\varepsilon_0\, dK_c$ ca. 1 for flexoelectricity (f ca. 10^{-20} C)

$e_s^2/\varepsilon\varepsilon_0\, dK_a$ ca. 10^{-4} for piezoelectricity (e_s ca. 10^{-12} C/m)

can be employed for comparisons of these mechanisms.

Flexoelectricity provides excellent electromechanical coupling (due to the small curvature elasticity K_c) and a linear response: polarization vs. curvature. Moreover, flexoelectricity provides increasing current with increasing stimulus frequency, and, as such, it is especially effective in the high frequency regime (see below).

3. Patch clamp technique as a tool for mechanosensitivity studies

Stress-sensitive ion channels might be the structural correlates for mechanosensitivity of natural membranes. Most experiments on stress-sensitive channels in such membranes have been performed using patch clamp methods in which micrometer size patches of membrane were isolated by giga-ohm seals at the tips of glass micropipettes (Sakmann and Neher (1983) for details of the techniques). In some cases these patches were excised from the cell membrane and the stress-sensitivity of channels in the patches were then studied. Channels and pores in artificial membranes have been studied using the pipette-dipping technique of Coronado and Latorre (1983). This allows the formation of model phospholipid membranes containing channel-forming proteins or peptides.

3.1. Application of static and pulsed membrane tension using aerostatic pressure

A pressure difference can be readily applied across either a natural or an artificial membrane patch via the contents of the glass micropipette (Guharay and Sachs 1984; Petrov et al. 1992). The resultant tension induced in the patch can be calculated from the Laplace law (1) providing that the patch location, geometry and radius are known. The problem of obtaining accurate estimates of these parameters was solved by Sokabe et al. (1991) by employing quantitative videomicroscopy. They showed that patches excised from chick skeletal muscles are located 8–15 μm from the micropipette tip, and that the membrane patch radius changes (i.e. decreases) with pressure. They also showed that the curvature of a patch changes its sign according to the sign of the applied pressure. Tension in the patch increases as the pressure is increased until the patch assumes a hemispherical shape. At this point the relationship between tension and pressure becomes linear. Thus, the first direct observations of the position of a membrane patch and of its shape have been made. Indirect observations of these parameters can be made from measurements of membrane capacitance using the method of Neher and Marty (1982). This method uses a patch clamp amplifier in combination with a lock-in amplifier and provides estimates of patch area changes (Gustin et al. 1988; Sokabe et al. 1991; Petrov et al. 1992). More accurate estimates have been obtained using a pseudo-random binary sequence technique (Clausen and Fernandez 1981; see also Joshi and Fernandez 1988) employing a software-based phase detector (Joshi and Fernandez 1988) and a phase tracker (Fidler and Fernandez 1989). Parallel electrical and optical observations of cell-attached patches of chick skeletal muscle indicate that membrane capacitance changes are exactly proportional to membrane area changes, i.e. about 0.7 μF/cm^2 (Sokabe et al. 1991). This proportionality is supposed to originate from a reversible in-flow of membrane lipid from the walls of the pipette into the patch. The reversibility of this phenomenon is considered to be due to the area elasticity of the cytoskeletal (spectrin/dystrophin) network associated with the patch; estimated to be 48.3 mN/m. There was a time delay of a few hundred ms after pressure was applied to the contents of the micropipette holding the patch before area/capacitance started to change. This delay was considered to be due to parallel elastic elements (i.e. cytoskeleton), since it almost disappeared after cytochalasin treatment of the patch (Sachs 1987). Somewhat similar data have been obtained from patches of locust skeletal muscle during application of slowly-rising pressure ramps. The maximum increase in patch area for a cell-attached patch was delayed by ~5 s with respect to the pressure maximum (Petrov et al. 1992; Fig. 5). Figure 5 demonstrates that SACs of locust muscle are sensitive to pressure change (resp. tension), not to membrane area change. Gustin et al. (1988) used a whole-cell technique, with optical monitoring of cell size and shape, for studying the effects of pressure (cell distension) on SACs of yeast cells. They showed that these SACs are also sensitive to membrane tension, with pressure inducing a steep rise of channel open probability P_{op}, which was inversely proportional to cell diameter; so a common dependence of P_{op} vs tension (calculated from the Laplace law) holds for all yeast cells. Perhaps, a dependence of P_{op} on tension calculated from the Laplace law holds for SACs in other cells. In support of this generalization, Sokabe et al. (1991) demonstrated that the sensitivity of channels in different patches of chick skeletal muscle did not vary in the same way a pressure was changed, but appeared to behave identically when sensitivity was assessed as a function of tension.

3.2. *Oscillating pressure and curvature variations. Registration of flexoelectricity*

A novel application of the patch clamp technique is to vary membrane curvature on a μm scale and, thus, to study the flexoelectric properties of natural and artificial membranes (Petrov et al. 1989, 1992, 1993). Optical observations have unambiguously shown that, under certain conditions, the curvature of a membrane patch changes in sign when the sign of applied pressure is changed. Membrane flexoelectricity is best studied with oscillating pressure whilst employing phase-sensitive detection of flexoelectric voltage (13) or current (14). A loudspeaker fed by a sine function generator or a loudspeaker-driven rubber bellows can be used for pressure generation (Fig. 6). Such studies are possible with either inside-out, outside-out or cell-attached membrane patches. A theoretical analysis of this approach is given below.

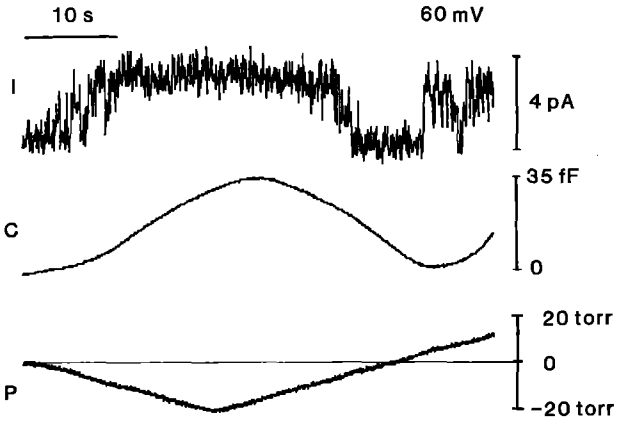

Fig. 5. Stress-activated channel current (I) and capacitance change (C) of a cell-attached patch of locust muscle membrane in standard locust saline in response to a slow pressure ramp (P). Pipette resistance 4.5 MΩ, pipette diameter 1.7 μm (estimated after Sackmann and Neher 1983), seal resistance 2 GΩ, patch capacitance $C_{fast}=3.45$ pF, $C_{slow}=0.8$ pF, access resistance 4.9 nS. Capacitance changes were monitored by the method of Neher and Marty (1982) using a combination of a List EPC7 patch clamp amplifier and a SR530 dual lock-in amplifier. A 5 kHz 50 mV (pp) carrier sine wave from the internal oscillator of SR530 was applied to the stimulating input of List amplifier (i.e. 5 mV (pp) applied to the patch). Pipette potential was 60 mV. Experimentally determined capacitance sensitivity (by decompensation of C_{fast} of List amplifier) was 2.7 mV/fF cf. theoretically calculated 2.777 mV/fF (at 50 mV/pA sensitivity of List and 100 mV sensitivity of lock-in amplifier, time constant 1 s). Current trace was 0.5 kHz filtered before plotting to supress the innitially fully compensated carrier wave. Stress activation of the channel followed closely pressure changes, activation thresholds were ca. −4 torr and 5 torr. In contrast, capacitance (i.e. area) changes were delayed with respect to the peaks and zeros of pressure by 5 s. This result demonstrates that SAC's of locust muscle react to tension, rather than to area change.

From the peak amplitude of capacitance increment (35 fF) which is very similar to the estimated initial value of the patch capacitance (estimation after Sakmann and Neher 1983) one can conclude that the patch is hemispherical in shape with a radius of curvature of 0.85 μm. With a pressure difference of −20 torr i.e. −2666 Pa Eq. (1) gives a patch tension of 2.3 mN/m (from Petrov et al. 1992).

Consider an oscillating aerostatic pressure $p_0 \sin(2\pi\nu t)$ applied to the contents of a patch pipette with a membrane patch at its tip. For a membrane curved by a static pressure difference p_0, its curvature radius, R, calculated from the Laplace law (1), would be $R=2T_m/p_0$. Now consider the application of static pressure to a flaccid, initially tension-free patch, for which the effects of induced tension obey Hooke's law (2). With $\Delta A/A=\pi h^2/\pi r^2$, where h is the height of the spherical segment which represents the patch surface at the amplitude value of pressure and r is the patch radius (i.e. spherical segment radius), and with $h^2=r^4/4R^2$ (valid for small h or large R):

$$R=(K_a r^2/2p_0)^{1/3}. \tag{27}$$

An approximate solution for the patch radius under the condition of oscillating pressure can be obtained by using an expression for the volume flow Q through a cylindrical pipe (i.e. the shank and shaft of the micropipette holding the patch) of radius r and length L (Loizjanskii 1987):

$$p_0-p_e=Q(8\eta L/\pi r^4), \tag{28}$$

where the pressure gradient is expressed by the difference of p_0, the pressure at the top of the micropipette and p_e, the pressure at the pipette tip (where the membrane is situated and η is the viscosity of water (electrolyte)). Since the hydraulic resistance (in the brackets of (28)) is inversely proportional to the fourth power of the micropipette radius, the dimensions of the micropipette tip are most important. The shaft of the pipette is approximated by a cylinder. The volume flow for a half period of a pressure oscillation is constrained by the volume displaced by the oscillating membrane patch simply as $Q=2V2\nu$, where V is the volume of the spherical patch (doubled as the

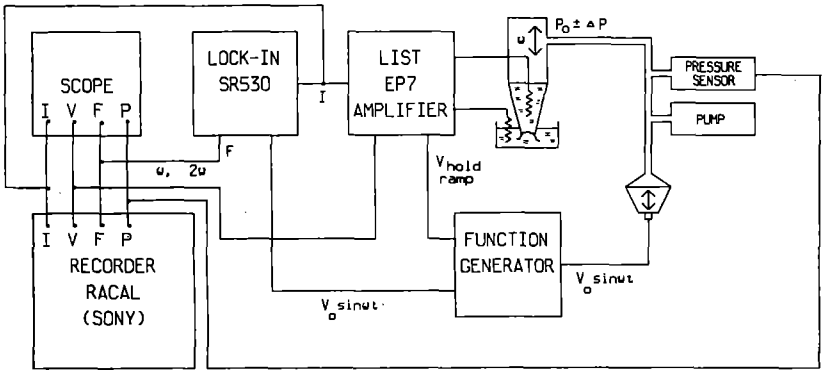

Fig. 6. Set-up for measuring flexoelectricity. Membrane curvature oscillations were excited by a loudspeaker-driven system fed by a function generator. Static pressure variations were produced by a reversible peristaltic pump. Pressure (P) was monitored by a pressure meter bridge based ona MPX100AP silicon piezoresistive pressure sensor. The membrane current (I) was amplified by a patch clamp amplifier and then passed to a dual lock-in amplifier (see Fig. 5, legend). Current, voltage, flexo- and pressure outputs were recorded on a 4 channel analog tape recorder. In some cases two of these signals were digitally recorded by a two channel PCM linked to a standard videorecorder

membrane is moved from negative to positive curvature) and v is the patch oscillation frequency. For small curvatures $2V=(\pi r^4/2R)$. Expressing the pressure p_e at the micropipette tip by the combined Laplace-Hooke law for an elastic membrane (Eq. (27)), (28) gives:

$$p_0-(K_a r^2/2R^3)=8\eta L v/R\,. \tag{29}$$

Equation (29) reduces to the static pressure situation when $v=0$. If the solution for R of (29) is a small addition to the static solution (27), then an approximate solution is obtained viz:

$$R=(K_a r^2/2p_0)^{1/3}+8\eta L v/3p_0\,. \tag{30}$$

Substituting for the elastic modulus $K_a=50$ mN/m (Sokabe et al. 1991), tip radius 1 μm, tip length 1 mm, pressure amplitude 1 torr = 133,3 Pa, water viscosity 1 cp = 10^{-3} J s/m^3, oscillation frequency 20 Hz, then $R=5.7$ μm + 0.4 μm = 6.1 μm. At 20 Hz the increase of radius of curvature of the membrane patch (i.e. the decrease of curvature $c=2/R$) due to the dissipation of pressure by viscous friction is slight. At 200 Hz the elastic and viscous resistance to patch curvature are similar. When K_a tends to zero, viscous friction will only limit the extent of patch curvature, although R from (30) would still be comparable to the membrane patch radius. Viscous friction would be substantial if the patch is located deep inside the tip of the micropipette and if the micropipette tip also contains cytoplasm (this is more likely with cell-attached patches). Nevertheless, patch curvatures could still be generated during pressure applications.

However, membrane tension changes the picture dramatically. A tension-free patch is therefore essential for the manifestation of substantial curvature during application of oscillating pressures. If a flat membrane patch is under lateral tension, then with a modest tension of $T_m=1$ mN/m and static pressure difference of 1 torr the Laplace law already yields $R=15$ μm (even when the area elasticity of the patch is neglected). With an oscillating pressure of amplitude p_0:

$$R=(2T_m+8\eta L v)/p_0\,, \tag{31}$$

i.e. the radius of curvature of the membrane patch will further increase. Tension originating from area elasticity also tends to decrease pressure-induced curvature, but to a lesser extent (compare the cubic root dependence on K_a in (29) to the linear dependence on T_m in (31)).

Estimates of membrane curvature amplitude can be obtained using CME (see 2.2.1). By measuring the amplitude of the second harmonic under voltage clamp, the amplitude of the capacitance change induced by pressure can be determined from (7). Bearing in mind that even during application of relatively low frequency pressure oscillations changes in membrane patch curvature are much faster than the time for lipid in-flow (typically 1 s), then the increase in patch area will be accompanied by a thinning of the membrane and $\Delta C/C_0=2\Delta A/A_0$, where C_0 and A_0 are the "resting" values for membrane capacitance and membrane area respectively. Using a geometrical expression for the area of a spherical cap, the radius of curvature R of the membrane patch can be expressed as

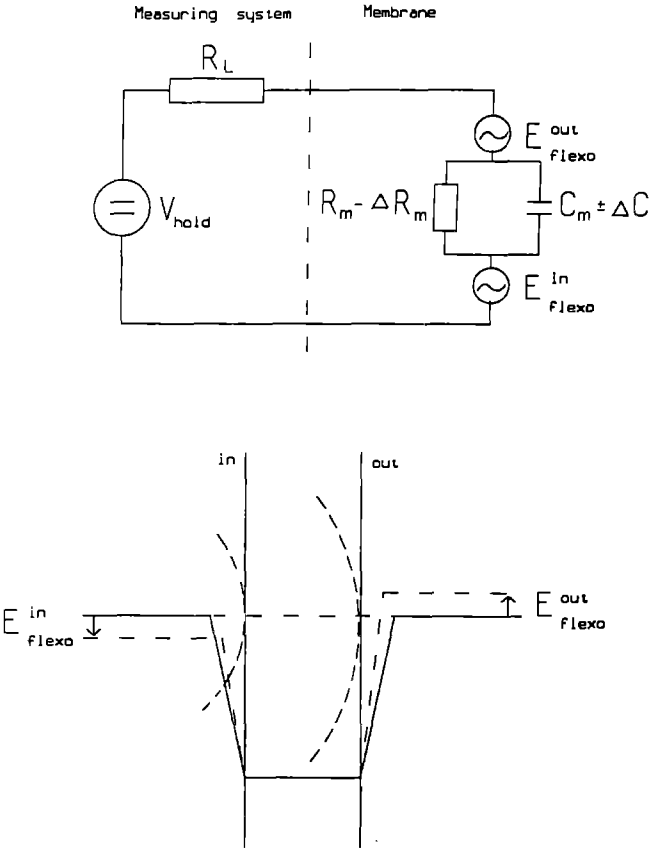

Fig. 7. Upper panel shows the equivalent circuit of an oscillating membrane connected to a system for recording flexoelectric responses. Lower panel shows a graph of the potential distribution across a planar and a curved membrane, related to the variation of surface dipole moments (see text). V_{hold} is the holding potential of a voltage clamp, R_L is the input resistance of the recording system, C_m is the membrane capacitance (and ΔC_m is its variation during oscillatory changes of membrane area) and R_m is the membrane resistance (and ΔR_m is its variation during channel opening). E^{out} and E^{in} are two e.m.f. generators which modulate the surface potentials of the two surface of a curved membrane (see lower panel for the case of a positive flexoelectric coefficient, negative surface charge and zero intramembrane field, i.e. zero current clamp). Since the two flexoelectric generators operate in counter-phase they can be combined as one generator to produce a potential difference of about 1 mV for a flexoelectric coefficient of 1×10^{-20} C and for a membrane radius of curvature of 1 μm.

follows (Petrov and Sokolov 1986):

$$R=(1+\Delta C/2C_0)\,(\Delta C/2C_0)^{-1/2}\,(d/4), \tag{32}$$

where d is the patch diameter.

Figure 7 gives the equivalent circuit for an oscillating flexoelectric membrane. From (13):

$$U_f=U_0\sin\omega t\,, \tag{33}$$

where U_0 is the flexoelectric voltage amplitude. In principle, this voltage could be measured at zero current under current clamp conditions. Alternatively, the current could be measured when the membrane is clamped at zero potential difference. As micropipette conductance σ_m (where seal conductance and membrane patch conductance are summed) and micropipette capacitance C_m (where membrane capacitance and micropipette stray capacitance are

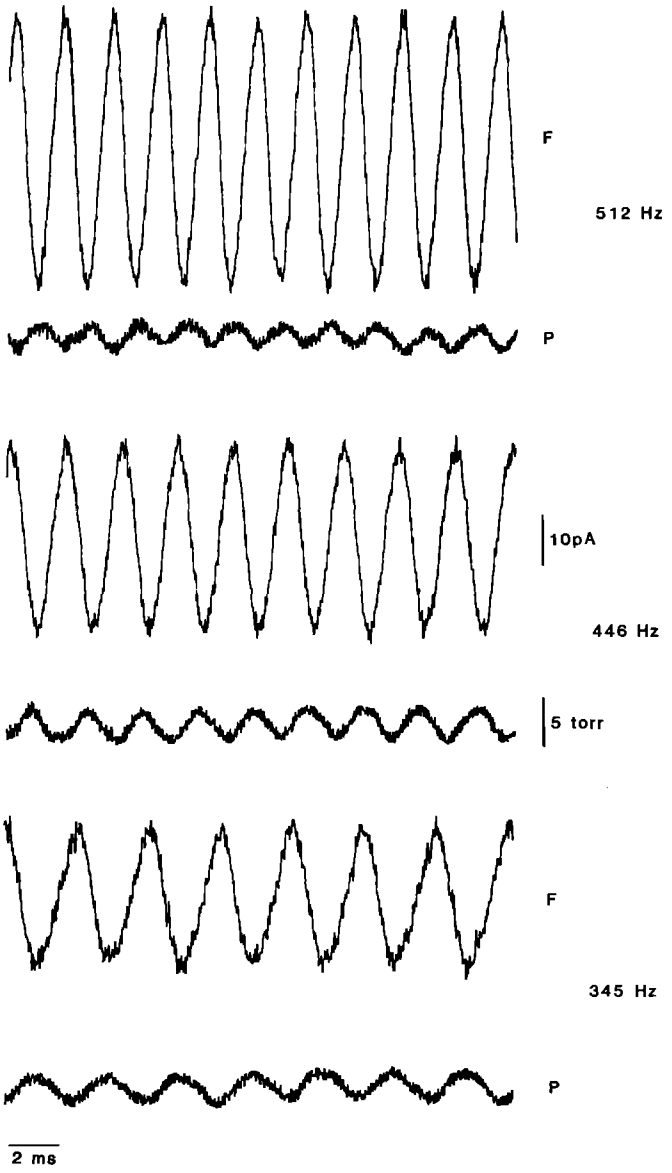

Fig. 8. Recordings of flexoelectric currents from an inside-out patch excised from locust muscle membrane in standard locust saline. Pipette resistance was 6.7 MΩ. Seal resistance was 0.5 GΩ. Patch capacitance components were $C_{fast}=7.5$ pF and $C_{slow}=0.8$ pF. Two types of K^+ channel were present in the patch (see Sect. 4.2.1). Upper traces, flexoelectric response (*F*) of the patch at 3 different frequences (345 Hz, 446 Hz and 512 Hz) in the high frequency range. Lower traces, driving pressure signals (*P*). Current bar of 10 pA and pressure bar of 5 torr apply to all measurements. Flexoelectric signals were strong enough to be directly recorded. No voltage dependence of the 1st harmonic was observed (i.e. patch oscillated around flat state). At 345 Hz, with 2.4 torr (pp) driving pressure a first harmonic flexoresponse of 9 pA (rms), phase −72° was observed. The control pick-up response after rupturing the patch and taking the pipette tip out of the saline was much lower (0.23 pA) and with completely different phase (170°)

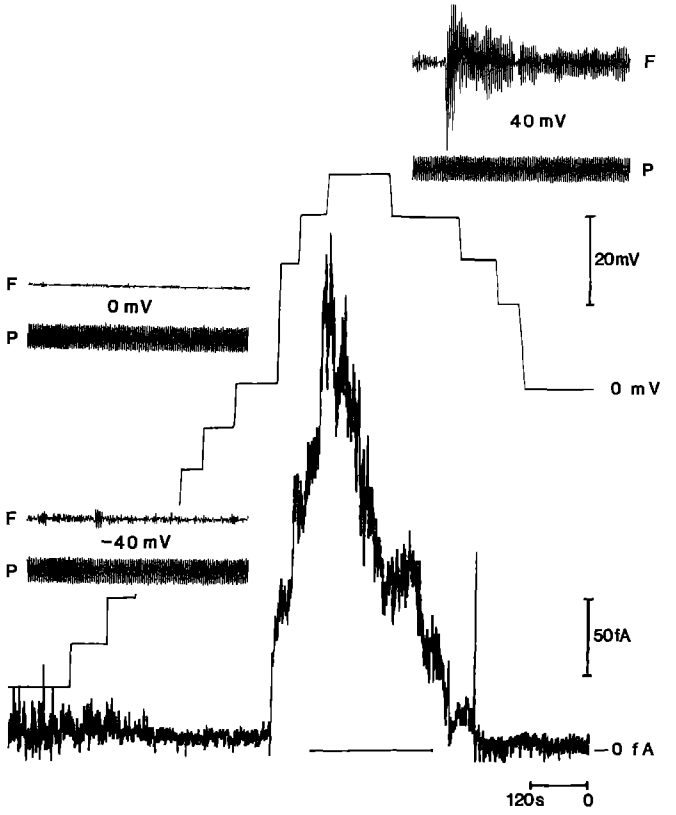

Fig. 9. Recordings of flexoelectric currents from a cell-attached patch of locust muscle membrane undertaken in standard locust saline. Voltage- dependent rms value of the flexoelectric response (*lower trace*) as a function of the pipette potential at the same moment of time (*upper trace*) (note that the time in this record runs from right to left). Low frequency (20 Hz, 10 torr (pp)) oscillating pressure. Pipette resistance was 9.1 MΩ, seal resistance was 1 GΩ. Insets show the pressure (*P*) and the actual shape of the flexoelectric response (*F*) as a function of time at −40 mV (30 fA rms, phase −140°), 0 mV (10 fa rms, phase −73°) and 40 mV (200 to 300 fA rms, phase −56°) pipette potential. Channel openings occurred mainly at positive pipette potentials. Individual openings and closings could be resolved at 40 mV by jumps in the amplitude of the flexoelectric signal. The overal current (not shown) has a d.c. component but the flexoelectric current (1st harmonic component) is a.c.-coupled

summed) are in parallel (Fig. 7), the total current will be:

$$I_f=\sigma_m U_0 \sin\omega t+\omega C_m U_0 \cos\omega t\ , \qquad (34)$$

i.e. it has an in-phase and a quadrature component with respect to the flexoelectric voltage. The second term in (34) increases linearly with frequency and becomes important at high frequencies. Its manifestation with an inside-out patch of locust muscle membrane is displayed in Fig. 8. The first term in (34) is important at low frequencies. It is coupled to the membrane conductance, thus its amplitude is sensitive to changes in conductance of the membrane patch, i.e. to openings and closings of channels. An example of this phenomenon in a cell-attached patch of locust muscle membrane is shown on Fig. 9.

4. Stress-activated and stress-inactivated ion channels and pores

Examples of stress-sensitive channels in natural membranes became abundant after their discovery by Guharay and Sachs (1984). However, the first examples of stess-sensitive channels were provided a decade earlier by studies of artificial membranes containing channel-forming peptides (see below).

4.1. BLMs containing channel-forming peptides

When pulses of pressure were applied to BLMs containing many gramicidin A molecules, Passechnik and Vitvizki (1975) showed that the average channel current induced by this peptide was stress-sensitive. A reversible decrease of current was obtained during pressure application, which was interpreted in terms of a stress-induced decay of the open state of the gramicidin-induced channels, thus providing the first example of a stress-inactivated artificial membrane channel. Later studies with this system (Flerov 1981; Passechnik and Flerov 1983; Passechnik 1983) involved application of pressure oscillations (2–10 Hz). These revealed harmonic components of the total number of channel openings and of the kinetic constants of recombination k_R and dissociation k_D of the gramicidin A conducting dimers. Dissociation was two times more sensitive to stress than recombination; it was also almost in-phase (9°) with the BLM stretching, while the recombination was phase-shifted by 109° (Flerov 1981). These results may be interpreted in terms of changes in membrane thickness by the open state of the channel (Eq. (23)): the length of the open gramicidin dimer may just fit the equilibrium BLM thickness (lipid extract from rabbit sarcoplasmic reticulum), but may exceed the thickness of a stretched BLM. Interestingly, the open state conductivity of gramicidin was unaffected by stretch.

Studies of synthetic lecithin (DPhL) bilayers containing oligopeptide toxins (microcystin, nodularin) from blue-green algae were made using the pipette-dipping technique of Coronado and Latorre (1983) by Petrov et al. (1991 a). These weakly biphilic and wedge-like toxin molecules may aggregate to form semi-toroidal, hydrophilic pores (Fig. 2 b). The pores formed by the toxins exhibited many conductive states (from 5 pS to >1000 pS). Tension-induced switching from low to high conductance states were observed when both positive and negative pressures were applied to a bilayer (Petrov et al. 1991 a; 1992). Assuming that the membrane bilayer area changes by a few percent during application of pressure (Sokabe et al. 1991), a mechanosensitivity coefficient of ~100 during switching from low to high conductance states could be inferred (Fig. 10). These studies show that membrane tension can modulate not only pore open probability but also the open pore conductance, a result which is in line with the theoretical model in Sect. 2.2.5. The stress sensitivity of these toxin pores is greater than that of a continuously stretched pore (18) because of the discrete nature of its conducting states. The results of these studies also demonstrate, contrary to the claims of Sokabe et al. (1991), that a pure lipid bilayer (i.e. without cytoskeleton) can sustain a lateral tension under a constant pressure difference. However, there could be one important difference between patches of natural and artificial membranes. In the former case the formation of a protein-glass seal would allow for lateral movement of lipids which would not be possible with pure lipid bilayers (see also Delcour et al. 1989).

4.2. Natural membranes. Stress-activated and stress-inactivated channels

4.2.1. Linear vs. quadratic models of channel gating. The first studies of native SACs were undertaken independently by Guharay and Sachs (1974) in tissue-cultured embryonic chick skeletal muscle and by Brehm et al. (1984) in innervated muscle of *Xenopus laevis*. Since then the number of cell types and tissues where SACs have been observed exceeds 30 (Morris 1990, Sachs 1989). It is possible to distinguish between SAAn (anion selective), SACat (cation selective), SAK (predominantly potassium selective), SACa (selective for calcium and other divalent cations), and SANon (non-selective or poorly selective between cations and anions) channels (Morris 1990).

Interestingly, apart from mechanically induced stress activation, the SACs of *E. coli* can also be reversibly activated by amphipatic local anesthetics (Martinac et al. 1990). The results are again interpreted in terms of a bilayer expansion accompanying the asymmetric amphipath adsorption (Markin and Martinac 1991). These observations support the view that a mechanical gating force can be transmitted to the channel by its surrounding lipids.

The stress-sensitivities of two potassium-selective channels in membrane of adult locust muscle have been recently studied (Petrov et al. 1992; Miller et al. prepared for publication). A plot of the log of the ratio of open probability/close probability of one of these channels (a 35 pS channel) as a function of applied pressure is shown in Fig. 11. The linear fit to this plot is obtained from the model of (20) and (21) and yields a slope of 0.0309 torr^{-1}, i.e. 2.32×10^4 Pa^{-1}. Assuming a pipette radius as 1.3 μm (estimated from the micropipette resistance (Sakmann and Neher 1983)) and using the Laplace law (1) to calculate membrane tension (assuming a hemispherical geometry for the membrane patch) (20) and (21) give an area increment ΔA_p for this channel of 2.8 nm^2. For comparison, other membrane channels display a total cross-sectional area of about 80 nm^2. ΔA_p for the 35 pS channel of locust muscle is only 3.5% of the total channel area, and thus completely feasible. During a step increase in tension there was an initial activation of several 35 pS channels in a cell-attached patch of locust muscle, but this activity was fully maintained for only 1–2 s. These observations are consistent with the idea of lipid in-flow (Sokabe et al. 1991) relaxing (but not to zero) the lateral tension in the membrane patch.

Attempts have been made to obtain a linear fit to the data of Guharay and Sachs (1974). Morris (1990) also used linear models to fit data from a variety of SACat and SAK channels after finding that both linear and quadratic models fit the experimental data equally well. In fact, a linear model provides a better fit for chick muscle SACat channel and snail neuron SAK channel, while a quadratic model fits data for frog lens SACat channel and snail heart SAK channel better then a linear model. Our linear fit to the log of the tension-dependent rate constant $k_{1,2}$ of chick skeletal muscle SACs (Fig. 8 of Guharay and Sachs 1974) yields a slope of 0.06 $\text{torr}^{-1} = 4.5 \times 10^{-4}$ Pa^{-1}. For a 2 μm hemispherical patch (Guharay and Sachs 1974) an

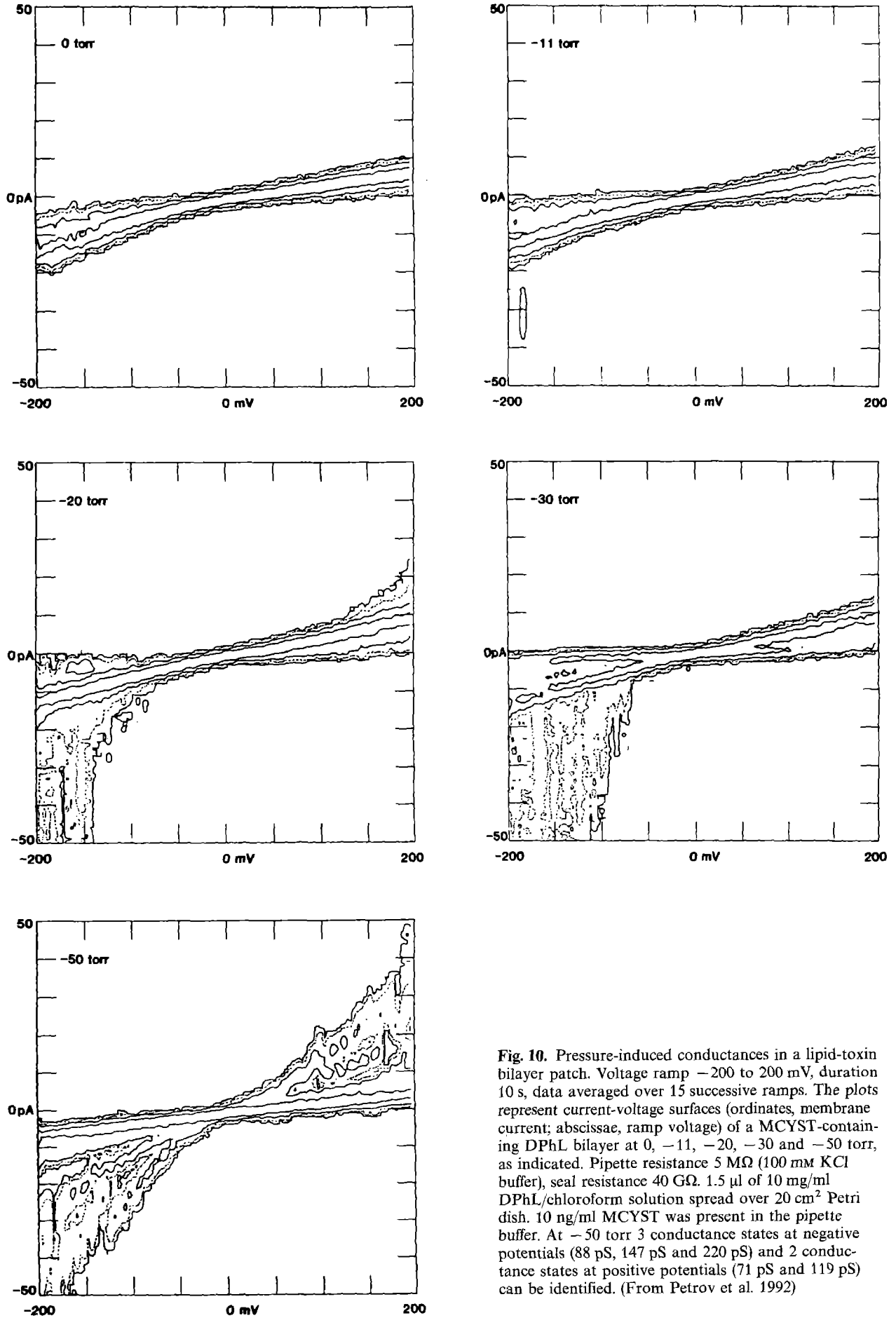

Fig. 10. Pressure-induced conductances in a lipid-toxin bilayer patch. Voltage ramp −200 to 200 mV, duration 10 s, data averaged over 15 successive ramps. The plots represent current-voltage surfaces (ordinates, membrane current; abscissae, ramp voltage) of a MCYST-containing DPhL bilayer at 0, −11, −20, −30 and −50 torr, as indicated. Pipette resistance 5 MΩ (100 mM KCl buffer), seal resistance 40 GΩ. 1.5 µl of 10 mg/ml DPhL/chloroform solution spread over 20 cm^2 Petri dish. 10 ng/ml MCYST was present in the pipette buffer. At −50 torr 3 conductance states at negative potentials (88 pS, 147 pS and 220 pS) and 2 conductance states at positive potentials (71 pS and 119 pS) can be identified. (From Petrov et al. 1992)

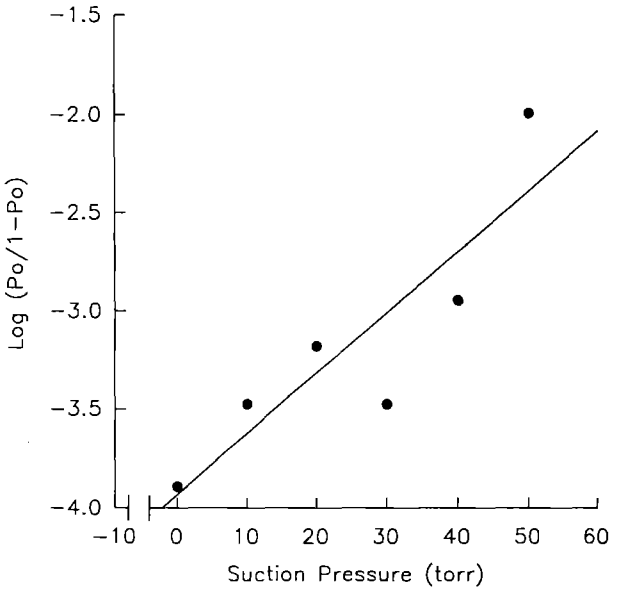

Fig. 11. Relationship between SAC open probability (P_0) and pressure. Cell-attached patch of locust muscle membrane with a 35 pS SA-channel. Both bath and patch pipette contained standard locust saline. Pipette resistance was 7.1 MΩ, seal resistance was 2 GΩ. Pipette potential was 0 mV. The data were low-pass filtered at 1 kHz. Values for P_0 were obtained from the area of the peaks of frequency distribution histograms of membrane currents (after Sokabe et al. 1991). Linear regression fit to data points has a slope of 0.0309 $torr^{-1}$ and an intercept of −3.93

area increment $\Delta A_p = 3.6\ nm^2$ was calculated for chick muscle channel, i.e. similar to the value for the 35 pS channel of locust muscle quoted above. Thus, the linear model states that channels exhibiting cross-sectional variation of the order of 3–5% during gating will be stress-sensitive.

Stress-inactivated channels have been observed in snail neurons and mammalian astrocytes. These channels are predominantly permeable to potassium (Morris 1990). They are usually inactivated at tensions below those needed to activate SA channels. The linear model predicts then a negative increment in the maximum cross-sectional area of an SI channel >5%. The presence of SICs and SACs in a membrane can result in a "notch-filter" performance, which would minimize K^+ permeability at certain tensions (Morris and Sigurdson 1989). In principle, a "band pass-filter" effect, which would maximize K^+ permeability at some tensions, might also be expected.

4.2.2. Failure of elicit macroscopic mechanosensitive currents and the role of cytoskeleton. Morris and Horn (1991) argued against a mechanosensitive role for SACs in snail nerve cell since they were unable to elicit macroscopic currents from such cells in response to mechanical stimuli. This lack of correspondence between the microscopic and macroscopic properties of these cells is possibly due to the presence of an intact cytoskeleton in the macroscopic studies (Fig. 1). As we have seen in Sec. 2.1.1, an intact cytoskeleton brings about a drastic attenuation in local membrane tension. The tension attenuation factor equals the ratio r/R of the mean distance between the attachment points of the cytoskeleton to the cell radius. This ratio is of the order of 1/100 for a whole cell and 1/10 for a 1 μm membrane patch. Additionally, a partial disruption of the membrane-cytoskeleton attachment is a probable event during patch formation. Disruption of actin-containing elements of the cytoskeleton by cytochalasin treatment leads to a profound increase (30 times) of the stretch-sensitivity of chick muscle SACs (Guharay and Sachs 1984). At a variance to Morris and Horn's results for a particular cell type several groups have now successfully recorded whole cell mechanosensitive currents in a variety of cell types (see Hamill et al. 1992).

In principle, all membrane channels which exhibit different cross-sectional areas in their open state and closed state are potentially mechanosensitive. In an intact cell membrane tension is partitioned between the cytoskeleton and the bilayer, but only the latter directly influences channel gating. This bilayer component of the tension is proportional to the mean distance between the attachment points of the membrane to the cytoskeleton (Sect. 2.2.1). Attenuation of the bilayer tension may explain the observations of rapid (i.e. in less than 0.5 s) and complete adaption of SACs in response to sustained mechanical stimulation (Hamill et al. 1992). During this time the redistribution of tension between the lipid bilayer attaining high local curvature and the cytoskeleton probably takes place. However, the possibility that components of the cytoskeleton might also influence channel gating cannot be ignored. For example, dystrophic muscle cells with a cytoskeleton that lacks normal dystrophin exhibit abnormal mechanosensitivity. However, non-pathological changes in the cytoskeleton, e.g. reducing the number of, and increasing the distance between, its attachment points to the bilayer may also influence channel gating (Morris and Horn 1991). The dismantling of the cytoskeleton during cell division might also be influential in this respect (Zhou and Kung 1992).

5. Flexoelectricity and dynamical strains sensing

Flexoelectricity occurs in pure lipid bilayers as well as in bilayers containing channels and pores. The question arises whether this phenomenon has any biological significance. Flexoelectricity may operate in channel-free lipid bilayer regions of biological membranes, although the presence of channels protein brings about some interesting new possibilities (see Sect. 3.2 and Fig. 8).

The stereocilia tips of hair cells are highly-curved membrane regions (Fig. 3). With a stereocilium diameter of 300 nm (Passechnik 1988) the tip curvature (2/R) is $13 \times 10^6\ m^{-1}$. During oscillations of a stereocilium this curvature would cyclically increase and decrease. Assuming a 10% curvature variation and a flexoelectric coefficient of 10^{-20} C (13), the change in curvature would result in a change of membrane potential of 1.5 mV. This membrane potential change would be concentrated in the tip of the stereocilium. There is experimental evidence that this region is the site of the mechanoelectric transducer (Hudspeth 1982, 1983). The stereocilium membrane is

concertinated at rest, but during stretch the folds will disappear (Fig. 3). These changes of curvature resulting from a stretch are an additional source of flexoelectricity. The value of 1.5 mV favorably compares to the known values of the hair cell sensitivity of 2 to 4×10^5 V/m (Howard et al. 1988), which yields a few mV change of the membrane potential at 10 nm displacement.

The flexoelectric generators of stereocilia are in parallel, so their total e.m.f would remain the same. However, the flexoelectric current, being proportional to the membrane area, would increase in proportion to the number of stereocilia that are activated in concert (14 and 34). With a tip area of $2\pi R^2 = 1.4 \times 10^{-9}$ cm^2 and a specific membrane capacitance of 1 μF/cm^2 (34) gives, at 1000 Hz oscillation frequency and a flexoelectric potential of 1.5 mV, a flexoelectric (displacement) current amplitude of 13 fA per stereocilium, i.e. 1.3 pA for a bunch of 100 stereocilia. This is a lower estimate in view of the possible additional flexoelectric current generated along the shaft of the stereocilium. The flexoelectric current is of greatest interest with high frequency stimuli, when it is largest, and when its linear growth with frequency would overcome the frequency-dependent decrease in amplitude of the imposed displacement of the stereocilium. With low frequency stimuli the conductive component of (34) becomes important, its value being directly dependent on the conductive states of the ion channels of the stereocilium membrane (Fig. 9).

Oscillations of the potential difference across a bilayer membrane may induce curvature oscillations in that membrane, i.e. converse flexoelectric effect. This has been observed in BLMs using stroboscopic interferometry (Todorov et al. to be published). Thus, further possibilities for participation of flexoelectricity in the active process of mechanoamplification (Passechnik 1988) may be discussed, inspired in particular by the fact that the curvature-generating flexoelectric mechanism may be fast enough.

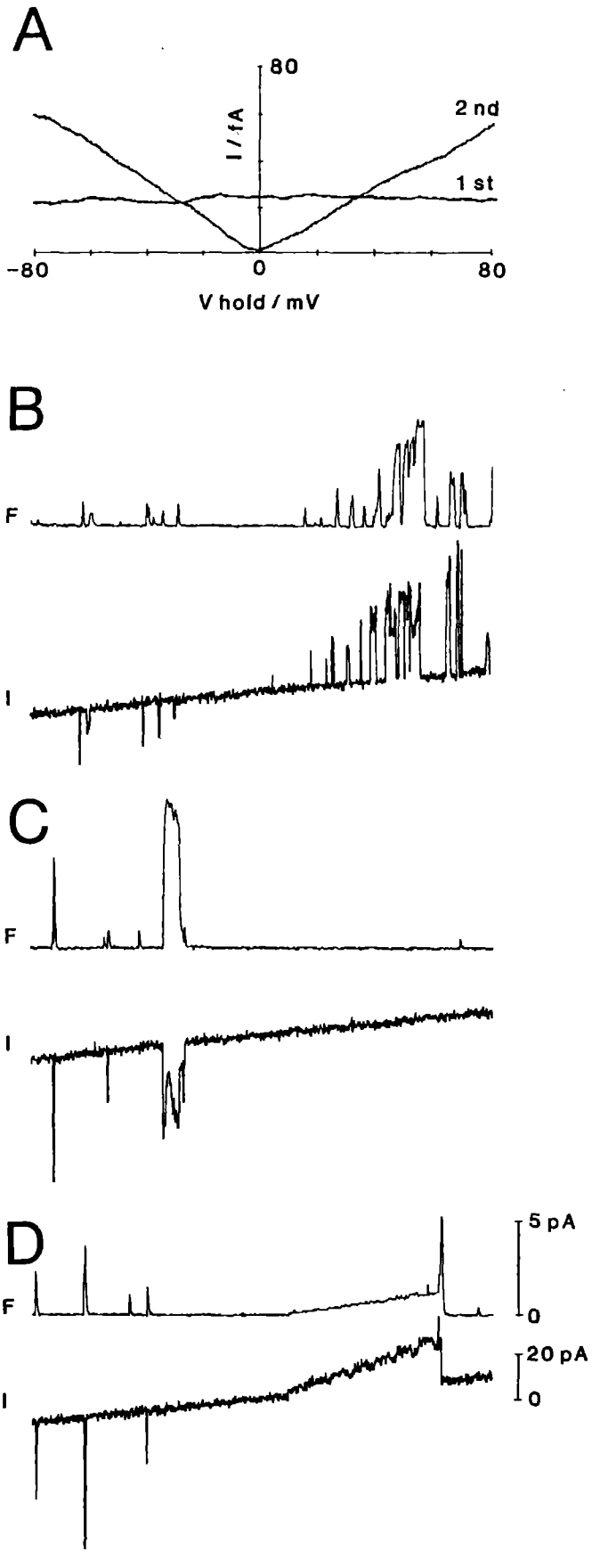

Fig. 12a–d. Flexoelectric responses recorded from a DPhL bilayer patch using a 150 mM KCl buffer and 20 Hz, 5 torr (pp) oscillating pressure. Pipette resistance was 1 MΩ, seal resistance was 0.5 GΩ. $A \pm 80$ mV voltage ramp was applied; total ramp time was 100 s. **a** First (1st) and second (2nd) harmonic of the current showing different dependencies on holding potential (±80 mV). The 2nd harmonic follows the theoretical expectation for a flat, symmetric patch by going to zero proportionally to the absolute value of pipette potential V_{hold}. From the slope of 2nd harmonic vs. voltage the curvature radius amplitude was estimated to be 5.2 μm and from the 1st (voltage-independent) harmonic a flexoelectric coefficient of 4.1×10^{-21} C was determined (see text). **b–d** Three successive voltage ramps applied to the same patch as in A, but in this case pores were present in the bilayer (induced by prolonged mechanical excitation). Lower traces are overall current (I) and the upper traces are its 1st harmonic amplitude (F). When no pore openings were present the 1st harmonic was low (25 fA rms) and voltage-independent. With pore openings, flexoelectric responses up to 30 pA rms in magnitude were observed (not shown)

6. Application to biomolecular electronics

The systems described above may serve as prototypes of molecular machines with both mechanical and electrical controls.

6.1. Switches

The microcystin/lipid bilayer system referred to above provides an example of a molecular ion conducting switch, which may be both tension- and voltage-gated (Fig. 10) (Petrov et al. 1991 a).

6.2. Sensors

Oscillating membranes at the tips of patch micropipettes may find an application as miniature flexoelectric sensors for ion and dipolar species, because the signal generated by such membranes may change dramatically following adsorption of such species onto the membrane surface. Such sensors would be analogous to acoustoelectric sensors, which are based on surface acoustic waves, but much more compact. In principle a micropipette bearing a membrane patch could be inserted into a cell. Another possibility would be to use the tip of the micropipette as a miniature microphone in order to study microacoustic emission at the level of the cell. Dramatic amplification of the flexoelectric response of the membrane continued at the tip of the micropipette could be achieved if the bilayer contained pores or open channels (Fig. 12). Amplification factors of 10^3 or more were already obtained.

7. Conclusion

The identification and localisation of stress-sensitive elements in cell membranes is an important task for future studies. No doubt, such studies will greatly be promoted by the recent discovery of the first molecular probe for selective blocking of mechanosensitive channels: amiloride (Hamill et al. 1992). Attention must be paid, however, to all the elements of the cell membrane complex (not just to some specific conductive sites) and to its collective mechanical and mechanoelectrical properties. 'In situ' studies of membrane protein channels by modern spectroscopy methods can provide information about the conformational changes during mechanical gating. Finally, important new concepts can emerge by the consistent application of liquid crystal physics and polymer physics to mechanosensitivity of natural and artificial membranes.

Acknowledgements. One of us (A.G.P.) gratefully acknowledges a long-time collaboration with Professor Alexander Derzhanski, PhD, DSc, in the field of liquid crystal properties of membranes. The authors thank British SERC, British Council and Bulgarian National Fund "Scientific Studies" (Project F19) for financial support.

References

Beresnev LA, Blinov LM, Kovshev EI (1982) On the possibility of ferroelectricity in biomembranes. DAN SSSR 265:210–213

Blumenfeld LA (1974) Problemi biologicheskoj fiziki. Nauka, Moscow

Bograchova TJ, Passechnik VI, Sokolov VS (1974) The influence of periodical stretch on the conductivity of modified bilayer lipid membranes. Study Biophys 42:75–76

Brasseur R (1991) Differentiation of lipid-associating helices by use of three-dimensional molecular hydrophobicity potential calculations. J Biol Chem 266:16120–16127

Brehm P, Kullberg R, Moody-Corbett F (1984) Properties of non-junctional acetylcholine receptor channel on innervated muscle of *Xenopus laevis*. J Physiol 350:631–648

Brochard F, Lennon JF (1975) Frequency spectrum of the flicker phenomenon in erythrocytes. J Phys 36:1035–1047

Clausen C, Fernandez JM (1981) A low cost method for rapid transfer function measurement with direct application to biological impedance analysis. Pfluegers Arch Eur J Physiol 390:290–294

Coronado R, Latorre R (1983) Phospholipid bilayers made from monolayers on patch-clamp pipettes. Biophys J 43:231–236

Delcour AH, Martinac B, Adler J, Kung C (1989) Modified reconstitution method used in patch-clamp studies of *Escherichia coli* ion channels. Biophys J 56:631–636

Derzhanski A, Petrov AG (1982) Multipole model of the molecular asymmetry in thermotropic and lyotropic liquid crystals. Mol Cryst Liq Cryst 89:339–360

Derzhanski A, Petrov AG, Pavloff YV (1981) Curvature-induced conductive and displacement currents through lipid bilayers. J Phys Lett (Paris) 42:L119–L122

Derzhanski A, Petrov AG, Todorov A (1989) Flexoelectricity of layered and columnar lyotropic phases. Bulg J Phys (Sofia) 16:268–280

Derzhanski A, Petrov AG, Todorov A, Hristova K (1990) Flexoelectricity of lipid bilayers. Liq Cryst 7:439–449

Duwe H-P (1989) Korrelationsanalyse thermischer Formfluktuationen von Vesikeln mittels schneller, digitaler Bildverarbeitung. Dissertation, TU Munich

Duwe H-P, Engelhardt H, Zilker A, Sackmann E (1987) Curvature elasticity of smectic A lipid bilayers and cell plasma membranes. Mol Cryst Liq Cryst 152:1–7

Duwe H-P, Eggl P, Sackmann E (1989) The cell plasma membrane as composite system of two-dimensional liquid crystal and macromolecular network and how to mimick its physical properties. Angew Makromol Chem 166/167:1–19

Evans EA, Hochmuth RM (1978) Mechanochemical properties of membranes. In: Kleinzeller A, Bronner F (eds) Current topics in membranes and transport, vol 10. Academic Press, New York, pp 1–62

Evans EA, Needham D (1986) Giant vesicle bilayers composed of mixtures of lipids, cholesterol and polypeptides. Faraday Discuss Chem Soc 81:267–280

Evans EA, Rawicz W (1990) Entropy-driven tension and bending elasticity in condensed-fluid membranes. Phys Rev Lett 64:2094–2097

Fidler N, Fernandez JM (1989) Phase tracking: an improved phase detection technique for cell membrane capacitance measurements. Biophys J 56:1153–1162

Flerov MN (1981) Mechanosensitivity and current-voltage characteristics of ion channels in bilayer lipid membranes. PhD Thesis, Moscow State University

Gruen DWR, Wolfe J (1982) Lateral tensions and pressures in membranes and lipid monolayers. Biochim Biophys Acta 688:572–580

Guharay F, Sachs F (1984) Stretch-activated single ion channel currents in tissue-cultured embrionic chick skeletal muscle. J Physiol 352:685–701

Gustin MC, Zhou X-L, Martinac B, Kung C (1988) A mechanosensitive ion channel in the yeast plasma membrane. Science 242:762–765

Hamill OP, Lane JW, McBride Jr DW (1992) Amiloride: a molecular probe for mechanosensitive channels. TiPS 13:373–376
Harbich W, Helfrich W (1979) Alignment and opening of giant lecithin vesicles by electric fields. Z Naturforsch 34a:1063–1065
Helfrich W (1973) Elastic properties of lipid bilayers: theory and possible experiments. Z Naturforsch 28c:693–703
Hladky SB, Haydon DA (1984) Ion movements in gramicidin channels. In: Bronner F (ed) Current topics in membranes and transport, vol 21. Academic Press, New York, pp 327–372
Howard J, Roberts WM, Hudspeth AJ (1988) Mechanoelectrical transduction by hair cells. Annu Rev Biophys Chem 17:99–124
Huang HW (1986) Deformation free energy of bilayer membrane and its effect on gramicidin channel lifetime. Biophys J 50:1061–1070
Hudspeth AJ (1982) Extracellular current flow and the site of transduction by vertebrate hair cells. J Neurosci 2:1–10
Hudspeth AJ (1983) Mechanoelectrical transduction by hair cells in the acousticolateralis sensory system. Ann Rev Neurosci 6:187–215
Joshi C, Fernandez JM (1988) Capacitance measurements. An analysis of the phase detector technique used to study exocytosis and endocytosis. Biophys J 53:885–892
Katchalski A, Curran PF (1965) Nonequilibrium thermodynamics in biophysics, Chapter 10. Harvard University Press, Cambrige Mass
Kwok R, Evans E (1981) Thermoelasticity of large lecithin bilayer vesicles. Biophys J 35:637–652
Lecar H, Morris CE (1993) Biophysics of mechanotransduction. In: Rubanyi GM (ed) Mechanoreception by the vascular wall. Futura Publ Co, Inc, Mount Kisco, NY, pp 1–11
Lennon JF (1977) Le scintillement de l'erythrocyte. Doctoral thesis, University Paris-Sud, Orsay
Litster JD (1975) Stability of lipid bilayers and red blood cell membranes. Phys Lett 53A:193–194
Loizjanskii LG (1987) Fluid and gas mechanics (in Russian). Moscow, Nauka
Markin VS, Martinac B (1991) Mechanosensitive ion channels as reporters of bilayer expansion. Biophys J 60:1120–1127
Matrinac B, Adler J, Kung C (1990) Mechanosensitive ion channels of *E. coli* activated by amphipaths. Nature 348:261–263
Meyer RB (1969) Piezoelectric effects in liquid crystals. Phys Rev Lett 22:918–922
Mitov MD, Faucon JF, Meleard P, Bothorel P (1992) Thermal fluctuations of membranes. Adv Supramol Chem 2:93–139
Morris CE (1990) Mechanosensitive ion channels. J Membr Biol 113:93–107
Morris CE, Horn R (1991) Failure to elicit neuronal macroscopic mechanosensitive currents anticipated by single-channel studies. Science 251:1246–1249
Morris CE, Sigurdson WJ (1989) Stretch-inactivated ion channels coexist with stretch-activated ion channels. Science 243:807–809
Neher E, Marty A (1982) Discrete changes of cell membrane capacitance observed under conditions of enhanced secretion in bovine adrenal chromaffin cells. Proc Natl Acad Sci, USA 79:6712–6716
Neumann E, Sowers AE, Jordan CA (eds) (1989) Electroporation and electrofusion in cell biology. Plenum Press, New York London
Ochs AL, Burton RM (1974) Electrical response to vibration of a lipid bilayer membrane. Biophys J 37:667–672
Olesen S-P, Clapham D, Davies PF (1988) Haemodynamic shear stress activates a K^+ current in vascular endothelial cells. Nature 331:168–170
Parisi M, Rivas E (1971) Transient conductance changes induced by pressure in artificial lipidic membranes. Biochim Biophys Acta 233:469–473
Passechnik VI (1972) Modelling of mechanoreception with the help of modified bimolecular membranes. 4th Internat Biophys Congress, Moscow 1972. Abstracts vol 4, E XVIa 5/9, pp 44–45
Passechnik VI (1974) Possible mechanism of functioning of the elementary mechanosensitive center. Biofizika (Moscow) 19:1020–1924
Passechnik VI (1977) The problem of energy transformation in mechanoreceptors. Biofizika (Moscow) 22:1024–1029
Passechnik VI (1983) Viscoelastic properties of biomembrane models and mechanoreception processes. DSc Thesis, Moscow State University
Passechnik VI (1988) Mechanisms of the hearing organ (in Russian). Acc Sci Techn VINITI. Human and Animal Physiol Ser 39:6–121
Passechnik VI, Bichkova EJ (1978) Piezoeffect, background conductivity and filtration coefficient of bilayer lipid membranes. Biofizika (Moscow) 23:551–552
Passechnik VI, Flerov MN (1983) Influence of the mechanical deformation of membrane on the parameters of the ion channel formed by gramicidin A. In: Bilayer lipid membranes. Far East Sci Center Acad Sci USSR, Vladivostok, pp 90–110
Passechnik VI, Sokolov VS (1973) Permeability change of modified bimolecular phospholipid membranes accompanying periodical expansion. Biofizika (Moscow) 18:655–660
Passechnik VI, Vitvizki VM (1975) Mechanosensitivity of the membranes modified with the pore-forming substances. Biofizika (Moscow) 20:332–333
Pastushenko VF, Petrov AG (1984) Electromechanical mechanism of pore formation in bilayer lipid membranes. Seventh School Biophys Membrane Transport, Poland, School Proc vol 2:69–91
Petrov AG (1975) Flexoelectric model for active transport. In: Physical and chemical bases of biological information transfer. Plenum Press, New York London, pp 111–125
Petrov AG (1978) Mechanisms of curvature-induced membrane polarization and their influence on some membrane properties. Studia biophysica 74:51–52; Microfiche 4:14–25
Petrov AG (1981) The problem of self-assembly of lipids and proteins into liquid crystalline membrane structures. Sixth School Biophys Membrane Transport, Poland. School Proc Wroclaw 1:116–145
Petrov AG (1984) Flexoelectricity of lyotropics and biomembranes. Nuovo Cimento 3D:174–192
Petrov AG (1986) Molecular physics and biophysical aspects of lyotropic liquid crystalline state of matter. DSc Thesis, Bulgarian Academy of Sciences, Sofia
Petrov AG (1988) Generalized lipid asymmetry and instability phenomena in membranes. Ninth School Biophys Membrane Transport, Poland, School Proc Wroclaw 2:67–86
Petrov AG (1992) Flexoelectricity of membranes and electric double layers. In: Jennings BR, Stoylov SP (eds) Colloid and molecular electrooptics. Inst Physics Publ. Bristol Philadelphia, pp 171–176
Petrov AG, Bivas I (1984) Elastic and flexoelectric aspects of out-of-plane fluctuations in biological and model membranes. Prog Surface Sci 16:386–512
Petrov AG, Derzhanski A (1976) On some problems in the theory of elastic and flexoelectric effects in bilayer lipid membranes and biomembranes. J Phys Suppl 37:C3-155–C3-160
Petrov AG, Derzhanski A (1987) Generalized asymmetry of thermotropic and lyotropic mesogens. Mol Cryst Liq Cryst 151:303–333
Petrov AG, Sokolov VS (1986) Curvature-electric effect in black lipid membranes. Dynamic characteristics. Eur Biophys J 13:139–155
Petrov AG, Seleznev SA, Derzhanski A (1979) Principles and methods of liquid crystal physics applied to the structure and functions of biological membranes. Acta Phys Pol A55:385–405
Petrov AG, Mitov MD, Derzhanski A (1980) Edge energy and pore stability in bilayer lipid membranes. In: Bata L (ed) Adv liquid crystal res appls. Pergamon Press, Oxford, pp 695–737
Petrov AG, Ramsey RL, Usherwood PNR (1989) Curvature-electric effects in artificial and natural membranes studied using patch-clamp techniques. Eur Biophys J 17:13–17
Petrov AG, Ramsey RL, Codd GA, Usherwood PNR (1991 a) Modelling mechanosensitivity in membranes: Effects of lateral tension on ionic pores in a microcystin-toxin containing membrane. Eur Biophys J 20:17–29

Petrov AG, Todorov AT, Bonev B, Blinov LM, Subachyus DB, Tsvetkova N (1991 b) Manifestation of ferroelectricity in lyotropics with chiral additives: Biomembranes' analogs. Ferroelectrics 114:415–427

Petrov AG, Usherwood PNR, Miller BA (1992) Mechano-electricity of guest-host membrane systems: lipid bilayers containing ion channels. Mol Cryst Liq Cryst 215:109–119

Petrov AG, Miller BA, Hrtistova K, Usherwood PNR (1993) Flexoelectric effects in model and native membranes containing ion channels. Eur Biophys J 22:283–300

Sachs F (1986) Biophysics of mechanoreception. Membr Biochem 6:173–195

Sachs F (1987) Baroreceptor mechanisms at the cellular level. Fed Proc 46:12–16

Sachs F (1988) Mechanical transduction in biological systems. CRC Crit Rev Biomed Eng 16:141–169

Sachs F (1989) In: Stein WD, Bronner F (eds) Cell shape: Determinants, regulation and regulatory role. Academic Press, New York, pp 63–92

Sachs F, Lecar H (1991) Stochastic models for mechanical transduction. Biophys J 59:1143–1145

Sackmann E (1978) Dynamic molecular organization in vesicles and membranes. Ber Bunsenges Phys Chem 82:891–909

Sackmann E (1983) Physical foundations of the molecular organization and dynamics of membranes. In: Hoppe W, Lohmann W, Markl H, Ziegler H (eds) Biophysics. Springer, Berlin Heidelberg, pp 425–457

Sackmann E (1984) Physical basis of trigger processes and membrane structure. In: Chapman D (ed) Biological membranes. Vol 5. Academic Press, London, pp 105–143

Sackmann E, Duwe H-P, Pfeiffer W (1989) On the biomembranes as composite lamellae of smectic A liquid crystal and macro molecular network: elastic properties, local and collective dynamics. Phys Scr T25:107–113

Sakmann B, Neher E (eds) (1983) Single-channel recordings. Plenum Press, New York

Sansom MSP (1991) The biophysics of peptide models of ion channels. Prog Biophys Mol Biol 55:139–235

Schmidt CF, Baermann M, Isenberg G, Sackmann E (1989) Chain dynamics, mesh size, and diffusive transport in networks of polymerized actin. A quasielastic light scattering and microfluorescence study. Macromolecules 22:3638–3649

Sokabe M, Sachs F, Jing Z (1991) Quantitative videomicroscopy of patch clamped membranes stress, strain, capacitance, and stretch channel activation. Biophys J 59:722–728

Szekely JG, Morash BD (1980) The effect of temperature on capacitance changes in an oscillating model membrane. Biochim Biophys Acta 559:73–80

Todorov AT, Petrov AG, Brandt MO, Fendler JH (1991) Electrical and real-time stroboscopic interferometric measurements of bilayer lipid membrane flexoelectricity. Langmuir 7:3127–3137

Waugh R, Evans E (1979) Thermoelasticity of red blood cell membrane. Biophys J 26:115–132

Zhou X-L, Kung C (1992) A mechanosensitive ion channel in *Schizosaccharomices pombe*. The EMBO J 11:2869–2875

Zeman K, Engelhard H, Sackmann E (1990) Bending undulations and elasticity of erythrocyte membrane: effects of cell shape and membrane organization. Eur Biophys J 18:203–209

Zilker A, Engelhardt H, Sackmann E (1987) Dynamic reflection interference contrast (RIC-) microscopy: a new method to study surface excitations of cells and to measure membrane bending elastic moduli. J Phys 48:2139–2151